DIGITALCOMMONS
@WAYNESTATE

Wayne State University

Wayne State University Dissertations

1-1-2011

Molecular mechanisms of snare assembly and expulsion of intravesicular contents in cell secretion

Leah Jiyoung Zhang
Wayne State University,

Follow this and additional works at: http://digitalcommons.wayne.edu/oa_dissertations

 Part of the Molecular Biology Commons, and the Physiology Commons

Recommended Citation
Zhang, Leah Jiyoung, "Molecular mechanisms of snare assembly and expulsion of intravesicular contents in cell secretion" (2011). *Wayne State University Dissertations.* Paper 299.

This Open Access Dissertation is brought to you for free and open access by DigitalCommons@WayneState. It has been accepted for inclusion in Wayne State University Dissertations by an authorized administrator of DigitalCommons@WayneState.

www.manaraa.com

MOLECULAR MECHANISMS OF SNARE ASSEMBLY AND EXPULSION OF INTRAVESICULAR CONTENTS IN CELL SECRETION

by

LEAH J SHIN-ZHANG

DISSERTATION

Submitted to the Graduate School

Wayne State University

Detroit, Michigan

in partial fulfillment of the requirements

for the degree of

DOCTOR OF PHILOSOPHY

2011

MAJOR: PHYSIOLOGY

Approved by:

_____

Advisor Date

_____

_____

_____

_____

_____

www.manaraa.com

© COPYRIGHT BY

LEAH J. SHIN-ZHANG

2011

All Rights Reserved

www.manaraa.com

DEDICATION

This work is dedicated to my family, especially to my late father.

www.manaraa.com

ACKNOWLEDGMENTS

First and foremost I would like to acknowledge Dr. Jena, my doctoral advisor, for his encouragement, support and for giving me the determination to finish my studies. From him, I was inspired to have a passion for science and I will be forever indebted for the opportunity he gave me, without which, I might never have pursued my doctorate.

I would also like to thank my committee members Dr. Dunbar, Dr. Walz and Dr. Stemmler for their advice and guidance in this journey. Each has challenged me to look at my studies from a different perspective, which has made me a better researcher.

In addition to my advisor and committee members, I am extremely thankful to my colleagues in the lab. I especially thank Dr. Won Jin Cho for his time in training and answering all of my questions. Without his help, I would have not been able to accomplish my research. I also want to express thanks to Dr. Jin-Sook Lee for her guidance and initial training in the lab and to Zhi Hui Chen for her support and inspiration to maintain high standards for myself. In addition to my own lab, I am grateful for the guidance of Dr. Jeremy Cook and his patience in teaching me CD spectroscopy.

I am also extremely grateful for the staff in the Department of Physiology. To Ms. Chris Cupps, for her reassurance and without whom, I would have never completed all my requirements. I cannot reiterate enough how vital her presence is to this program and to the students of Physiology. To Ms. Sonya Bell, Ms. Linda McGraw and Ms. Joanne Kaiser for their support in multiple facets throughout the years, without which, I would have not been able to complete my projects. And to the rest of the Physiology department, to the professors for their outpouring of knowledge that has made me a better student, researcher and scientist, and to my fellow students for their

www.manaraa.com

understanding and support, I thank you.

I would also like to thank my mother (Soonock M. Shin) and late father (Jay Shin) for instilling in me the value of hard work and determination. To the rest of my family and especially my husband, Benjamin Zhang, for the love and encouragement along the way, I am always grateful.

This work is supported by research grants NSF CBET-0730768, NIH NS-39918 and Wayne State University Research Enhancement Program.

www.manaraa.com

TABLE OF CONTENTS

www.manaraa.com

www.manaraa.com

www.manaraa.com

LIST OF FIGURES

www.manaraa.com

www.manaraa.com

LIST OF TABLES

www.manaraa.com

CHAPTER 1

BACKGROUND

Overview of Cell Secretion

Elucidating the complexities of microscopic cellular systems is a major objective of scientific research in biology. Seemingly innocuous alteration to cellular operations can have an enigmatic impact on human biological activity as a whole. Cell secretion is one such mechanism that has enormous influence on numerous physiological processes. For example, the release of digestive enzymes, neurotransmitters, and hormones are employed through secretion, utilizing the molecular machinery referred to as porosomes (Jena 2009; Trikha et al., 2010). In exocrine pancreas (Schneider et al., 1997; Cho et al., 2002a; Jeremich et al., 2003), growth hormone cells of the pituitary (Cho et al., 2002e), chromaffin cells (Cho et al., 2002f), neurons (Cho et al., 2004, 2007, 2008; Siksou et al., 2007), and in other cell types, the function, morphology, and composition of the porosome has been demonstrated, and the structure has been functionally reconstituted into artificial lipid membrane. A porosome-like "canaliculi system" in human platelets (White & Clawson 1980; White 1999), for the precise and regulated docking, fusion, and release of intravesicular contents from these cells has also been demonstrated. Interestingly in Nature, even single-cell organisms have developed specialized and sophisticated secretory machinery, such as the secretion apparatus of Toxoplasma gondii (Joiner & Ross 2002), the contractile vacuoles in paramecium (Hausmann & Allen 1997), or the various types of secretory structures in bacteria (Kubori et al., 1998). These studies provide support that these structures and the mechanism of cell secretion is conserved and ubiquitous throughout species.

Investigation of cell secretion through conserved membrane structures

www.manaraa.com

(porosomes) has altered former exocytotic paradigms (Jena 2011). Previously, it was believed that exocytosis occurred through complete incorporation of vesicular membrane with the cell plasma membrane. While this theory postulated a possible mechanism for cellular release, it also raised a number of questions; for example, the conundrum as to why partially empty vesicles accumulate following cell secretion. Also, how could the cell utilize this method of secretion without growing exponentially in size due to the incorporation of vesicles into its membrane? And how could the cell control the amount released if vesicles had to discharge all their contents once they began to fuse with the plasma membrane? The second query was rationalized by the conjecture that compensatory endocytosis would follow exocytosis to account for the added membrane. However, a full understanding of the molecular mechanism of cell secretion required the direct observation of such events. It was not until the advent of Atomic Force Microscopy (AFM) and its near nanometer resolution of the dynamics of cell secretion that the mechanism of this process was confirmed (Kelly et al., 2004).

The story of cell secretion initially began with the discovery of *N*-ethylmaleimide-sensitive factor in the promotion of transport vesicle fusion with golgi (Malhotra et al., 1988). Subsequent discovery of SNARE proteins (Oyler et al., 1989; Bennette et al., 1992; Trimble et al., 1988) and their involvement in membrane fusion provided further support for a highly regulated cell secretory process. The presence of secretory machinery has also been suggested by electron micrograph (EM) images depicting cell membranes before (Figure 1A) and after (Figure 1B) secretion stimuli. Following the secretory stimulus, EM data depicts no change in the number of vesicles, but more importantly it also demonstrates the appearance of partially empty vesicles (Figure 1B & C). If complete incorporation of vesicles with the plasma membrane were the method

www.manaraa.com

by which cells secrete their intravesicular contents, then incomplete release of vesicular cargo would not be observed (Cho et al., 2002a). Instead, secretion would be synonymous to an all-or-none event in which vesicle numbers would decrease after stimuli and total intravesicular contents would be released to the extracellular medium. Empty or partially-filled vesicles (Figure 1C) would not accumulate within cells.

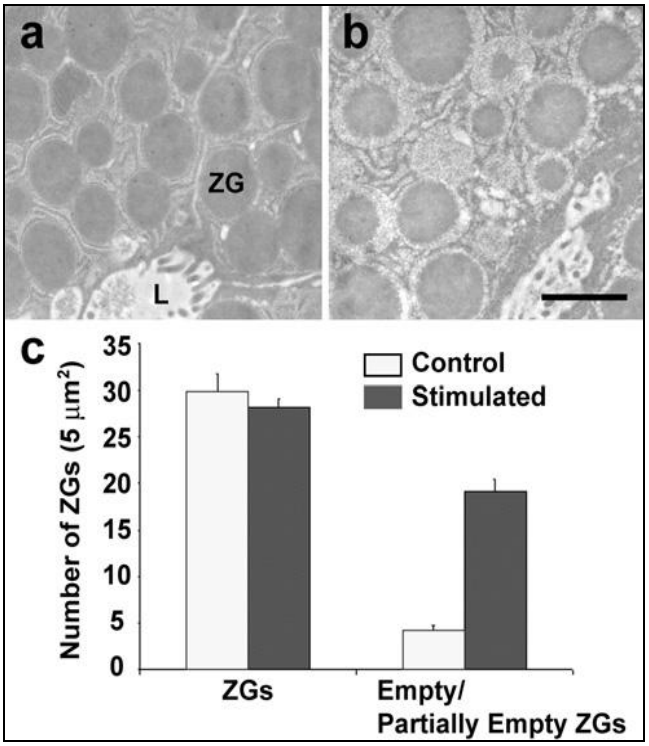

Figure 1. Electron micrographs of resting (A) and stimulated (B) pancreatic acinar cells. (C) The number of zymogen granules before and after stimulation remains unchanged. (D) The number of partially empty ZGs increases following stimulation. (Cho et al., 2002a)

These findings were substantiated by AFM studies on pancreatic acinar cells. Isolated live pancreatic acinar cells were imaged using AFM before and after simulation to secrete (Figure 2B-D). AFM data indicated that vesicles, located just below the surface of apical membranes, initially swelled or increased in size when a secretory

www.manaraa.com

stimulus was applied (Figure 2C) followed by a decrease in vesicle diameter, demonstrating release of intravesicular contents (Figure 2D). Immunoblot analysis of the secreted products confirmed the secretion of α-amylase from these cells (Figure 2E). Additionally, vesicle number did not change following a secretory stimulus. These results confirmed the earlier EM study findings, but above all demonstrated, for the first time, secretory events in live cells (Kelly et al., 2004).

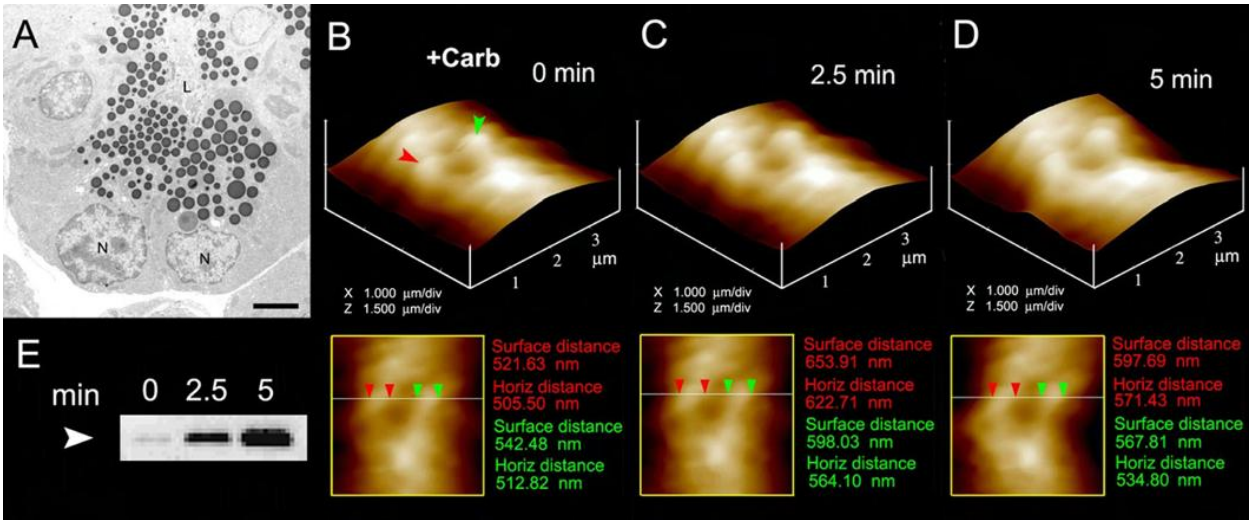

Figure 2. Electron micrograph confirming the presence of pancreatic acinar cells Bar = 2.5 µm (A). (B-D) Apical surface images of pancreatic acinar cells depicting the presence of secretory vesicles before (B) and after (C&D) the secretory stimulus, 1 µM carbachol (Carb), was applied. (E) Immunoblot analysis of secretory products from pancreatic acinar cells imaged in B-D. (Kelly et al., 2004)

Considered perhaps the preeminent discovery within this process was the discovery of the porosome (Schneider et al., 1997). Porosomes are structures at the cell plasma membrane by which cells can release their intracellular contents to the extracellular environment (Figure 3B) (Cho et al., 2005a). It has been demonstrated that secretory vesicles transiently dock and fuse at the porosome base during cell

www.manaraa.com

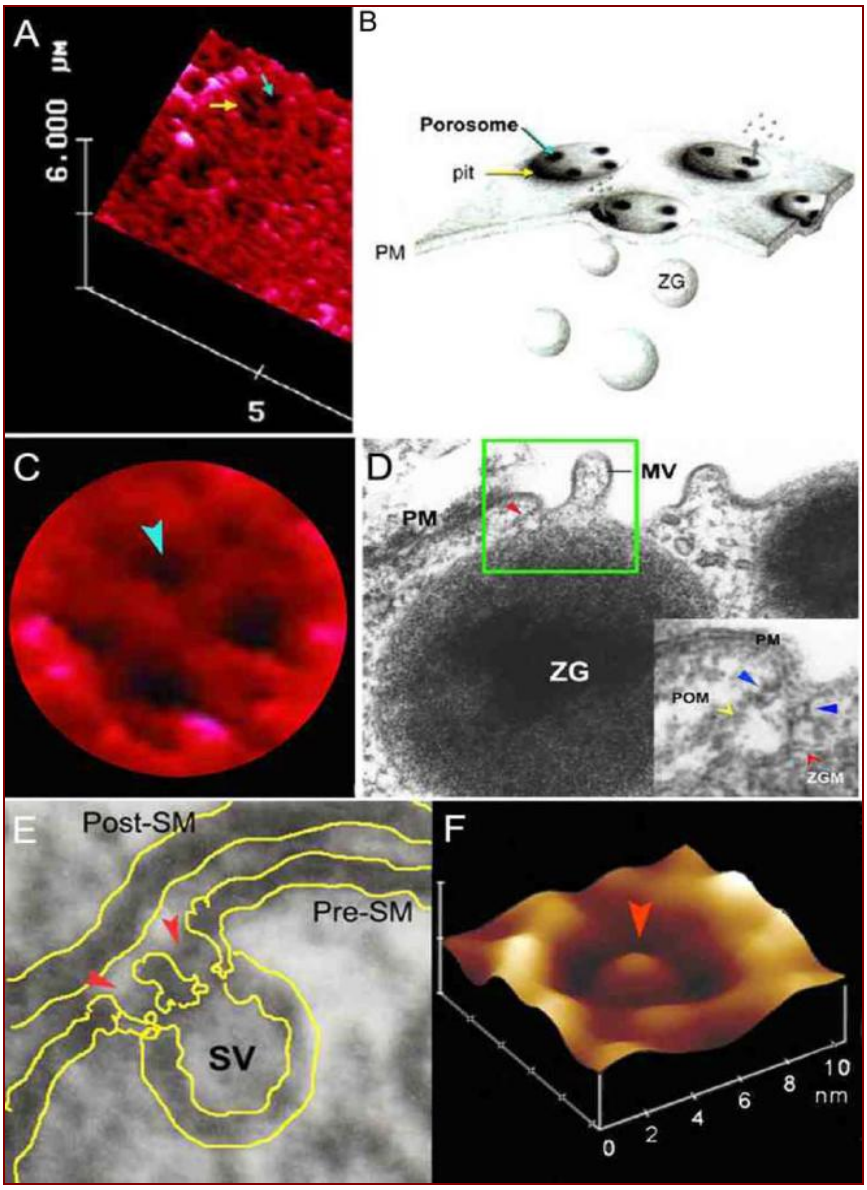

Figure 3. (A) AFM micrograph depicting pits (yellow arrows) and porosomes (blue arrows) at the apical plasma membrane of a pancreatic acinar cell. (B) Cartoon depiction of porosomes at the cell plasma membrane (PM). (C) High resolution AFM image showing a single pit with four porosomes within it. (D) Electron micrograph depicting porosome (red arrow) next to microvilli (MV) with expanded insert. (E) Close up EM image depicting a pre-synaptic membrane (SM) and associated synaptic vesicle (SV). (F) AFM micrograph of neuronal porosome. (Cho et al., 2005a)

secretion (Cho et al., 2005a). Proteins at the vesicle membrane, termed v-SNAREs (or secretory vesicle-associated membrane protein, VAMP) interact with t-SNAREs

www.manaraa.com

(comprised of SNAP-25 and syntaxin) located at the porosome base (Figure 4) (Jena 2003; Jeremic et al., 2003). These proteins associate to bring opposing vesicle and cell

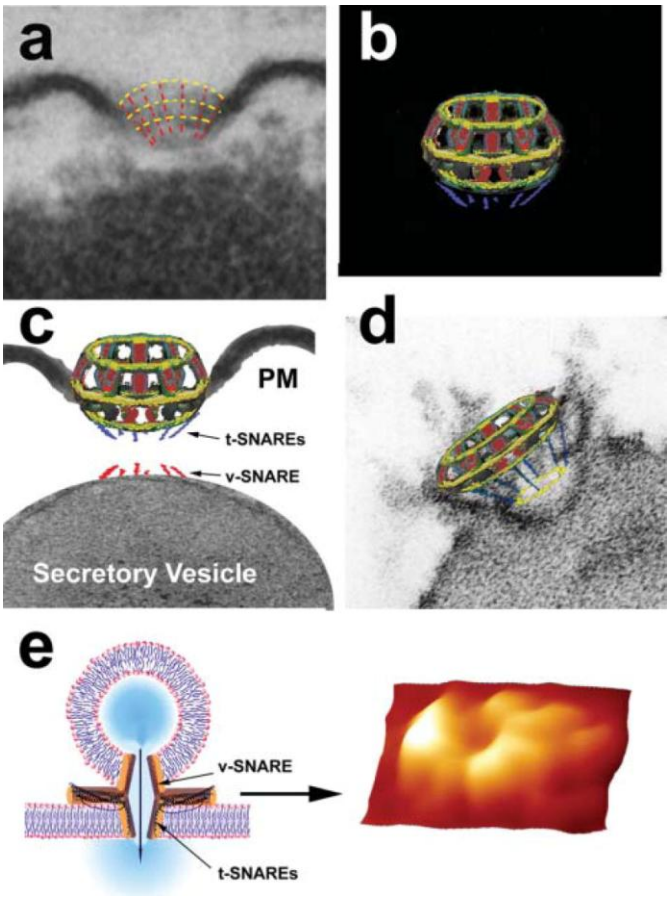

Figure 4. The fusion pore complex. (A) Electron micrograph of fusion pores isolated from rat pancreatic tissue with drawn in structure for clarity. (B) Schematic of the basket-like structure of the fusion pore depicting the presence of t-SNAREs (C) at its base (shown in blue) and its subsequent association with v-SNAREs at the zymogen granule membrane. (D) t- and v-SNAREs bring the cell membrane and zymogen granule membrane into closer proximity and associate in a circular array (yellow ring) to establish membrane continuity. (E) When v-SNARE reconstituted liposomes associate with t-SNARE reconstituted lipid bilayer, they form a circular array as shown by AFM. (Jena et al., 2003)

plasma membranes into close proximity, approximately 2.8Å, for subsequent establishment of calcium-mediated membrane continuity (Jeremic et al., 2004). As

www.manaraa.com

vesicle and cell membranes approach one another via SNARE complex assembly, fusion of the cell membrane to vesicle membrane to form a continuous channel requires the presence of calcium. Once fusion of the vesicle with the plasma membrane is achieved, intravesicular contents are expelled by way of vesicle swelling (Kelly et al., 2004). Following expulsion, the SNARE complex dissociates with the assistance of a soluble ATPase, known as *N*-ethylmalemide sensitive factor (NSF) (Jeremic et al., 2006). Although much about secretion has been discovered in the last 10 to 20 years, the exact molecular dynamics of this highly regulated process is incompletely understood.

Clinical Significance of Cell Secretion

Secretion and membrane fusion are fundamental cellular processes regulating ER-Golgi transport in protein maturation, plasma membrane recycling, cell division, sexual reproduction, acid secretion, and the release of enzymes, hormones and neurotransmitters, to name just a few. It is therefore no surprise that defects in secretion and membrane fusion give rise to diseases like diabetes, Alzheimer's, Parkinson's, acute gastroduodenal diseases, gastroesophageal reflux disease, intestinal infections due to inhibition of gastric acid secretion, biliary diseases resulting from malfunction of secretion from hepatocytes, polycystic ovarian disease as a result of altered gonadotropin secretion, and Gitelman disease associated with growth hormone deficiency and disturbances in vasopressin secretion. Understanding cellular secretion and membrane fusion will therefore help not only to advance our understanding of these vital cellular and physiological processes, but in the development of drugs to help ameliorate secretory defects (Jena 2004).

Similarly, disregulation of secretory processes, specifically SNARE mutations

www.manaraa.com

which disrupt secretion, can lead to impaired neuronal secretion (Fergestad et al., 2001), down regulation of vesicle trafficking pathways involved in secretion (Sprecher et al., 2005), and inhibition of hormone release (Jeans et al., 2007). In humans, a mutation in the gene encoding for SNAP-29, a protein involved in intracellular vesicle trafficking, results in CEDNIK (cerebral dysgenesis, neuropathy, ichthyosis, and keratoderma) syndrome. This disease is characterized by neurological and dermatological pathologies (Sprecher et al., 2005). Patients suffer from symptoms that range in severity, including delayed mental development, seizures, and even death (Sprecher et al., 2005). An alteration in gene expression typically accompanies diseases such as schizophrenia. In this disorder, proteins that regulate the pre-synaptic functional gene group (PSYN) are down regulated, effecting the expression of *N*-ethymalemide sensitive factor (NSF) and synapsin II (Mirnics et al., 2000). NSF and synapsin II are proteins involved in the secretory pathway; therefore, this study demonstrates yet another association between cell secretion and disease states.

Recently, studies have shown that non-structural membrane lipids such as lysophospatidylcholine (LPC) are also involved in secretory processes including secretion of atrial naturatic peptide (ANP) (Han et al., 2003) and endothelin-1 (Jougasaki 1992). The endogenous release of LPC is in response to ischemia (Han et al., 2003). LPC has been shown to inhibit the release of ANP in a dose-dependent manner through its effects on phosphoinositide 3-kinase and protein kinase-C pathways (Han et al., 2003). Because ANP typically acts as a vasodilator in response to high blood pressure (Baxter et al., 1988), these findings suggest that LPC may play a role in the progression of hypertension (Han et al., 2003). Cultured vascular endothelial cells when incubated with LPC, derived from oxidized low-density lipoproteins, cause a

www.manaraa.com

decrease in endothelin-1 secretion to counter vasoconstriction due to arthrosclerosis (Jougasaki 1992). Both studies indicate that LPC has effects on secretory pathways, specifically on inhibition of hormone secretion.

On account of the finding that LPC levels are also elevated in some cancers (for example in breast and ovarian cancers) (Sutphen et al., 2004; Fang et al., 2000), it follows that secretory processes can be altered by disease pathologies and could be possible targets for treatment. Lysophospholipids, specifically lysophosphatidic acid (LPA), lysophosphatidylserine (LPS), and sphingosylphosphorylcholine (SPC), are involved in calcium release pathways in ovarian as well as breast cancer cells (Xu et al., 1995). Their involvement in these pathways has correlations to cancer progression. Using mass spectrometry analysis of ovarian patients' blood samples, it was demonstrated that LPC levels are significantly higher in pre-operative patients (Stuphen et al., 2004). These levels were also significantly increased in early stage patients over controls (Stuphen et al., 2004). Highly aggressive cancer cells express the enzyme monoacylglycerol lipase (MAGL), which is capable of converting monoglycerides into a number of fatty acid derivatives, including lysophospholipids (Nomura et al., 2010). This lipogenetic pathway is then coupled to a lypolytic pathway employed by aggressive cancer cells to support their malignancy (Nomura et al., 2010). Since lysophospholipids play a role in both cancer and secretory processes, cancer progression could contribute to the disregulation of cell secretion.

Since cell secretion is an integral mechanism utilized by all secretory cells, investigation into its complexities is vital. Not only can its disruption lead to diseases (for example CEDNIK syndrome) (Sprecher et al., 2005), the mechanism of secretion itself can be affected by disease pathologies (such as in schizophrenia) (Mirnics et al.,

www.manaraa.com

2000) and circuitously through LPC in cancer. Cancer's potential links to cell secretory processes draws attention to the suggestion that other disorders could also ultimately be linked to impaired secretion. Because there are a myriad of disorders that are shown to have influence on secretion, the critical importance of studying this mechanism is further supported for expanding knowledge base and for disease therapies.

The Porosome

Acinar cells of the exocrine pancreas are polarized cells, which secrete digestive enzymes into the small intestine upon stimulation by a secretory stimulus. It is in these cells that the porosome or the secretory portal in cells was first observed (Schneider et al., 1997). Isolated live acinar cells, imaged by AFM, depict in real time the presence of circular pits approximately 0.4-1.2 μm in diameter at the apical membrane of these cells. Each pit also contains 3-4 smaller, cone-shaped depressions (porosomes) approximately 100-180 nm in diameter and 15-35 nm in height or depth (Figure 3A, B, C) (Cho et al., 2005a). Upon the addition of the secretagogue, mastoparan (a peptide derived from wasp venom), the cone-shaped depressions increase in size 25-45% with a reestablishment of resting size once secretion is terminated (Schneider et al., 1997). Reciprocally, introduction of cytochalasin B (a fungal toxin that inhibits secretion) to an acinar cell preparation causes a decrease in depression size and secretion (Schneider et al., 1997). In addition to these investigations, the existence of the porosome is confirmed in neuroendocrine cells (Cho et al 2002e; Cho et al., 2002f), neurons (Cho et al., 2004), and astrocytes (Lee et al., 2008).

To validate that these pores were indeed the structures by which cells secrete their intracellular contents, immuno-AFM experiments were performed using gold-

www.manaraa.com

conjugated antibody to acinar cell secretory products, specifically to amylase in case of pancreatic acinar cells (Cho et al., 2002b), and growth hormone in case of growth hormone secreting pituitary cells (Cho et al., 2002f). AFM images (Figure 5) depict

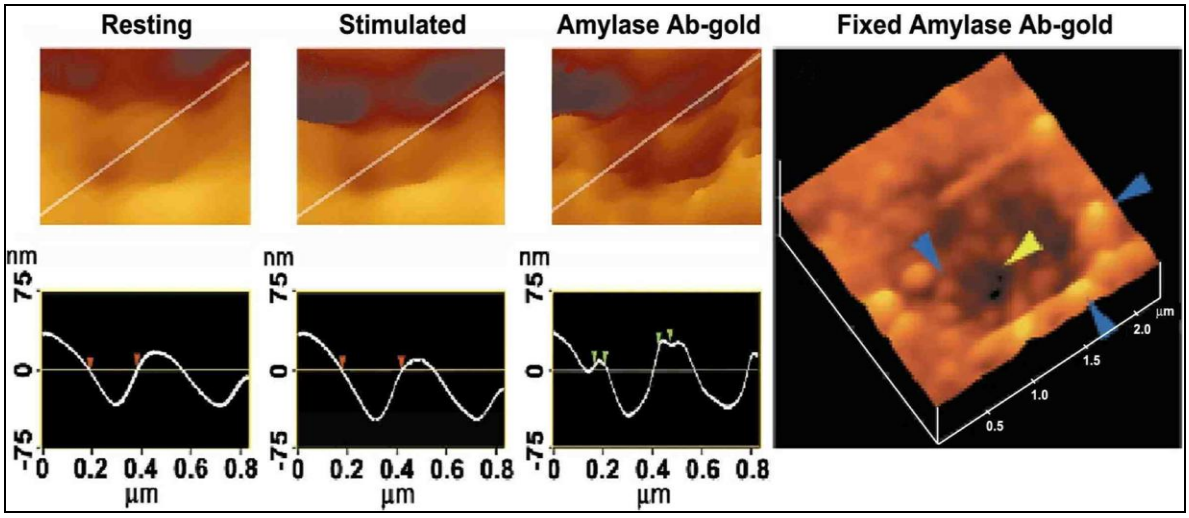

Figure 5. Porosome images and profiles before and after stimulation for secretion. Exposure of cells to gold-congugated antibody against amylase (blue arrowheads) shows their localization around pores (yellow arrow). (Jena 2008)

localization of these antibodies to the depressions or porosomes following a secretory stimulus. Once secretion is stimulated, zymogen granules (ZGs), vesicular bodies found in pancreatic acinar cells, dock and transiently fuse to the base of porosomes at the apical plasma membrane. Granules then swell, enabling the regulated expulsion of their contents, through the porosome opening. Therefore, detection of secretory products at the porosome and confirmation of their presence was substantiated by the use of gold-conjugated antibodies in these AFM investigations (Cho et al., 2002b).

The morphology of the pancreatic porosome complex has been further evaluated using transmission electron microscopy (TEM) (Jeremic, et al., 2003). TEM studies

www.manaraa.com

confirm the porosome to possess a cup-shaped structure, with similar dimensions as determined from AFM measurements. Additionally, TEM micrographs demonstrate pancreatic porosomes to exhibit a basket-like morphology, with three lateral and a number of vertically arranged ridges. A ring at the base of the complex is further identified (Jeremic, et al., 2003), and is hypothesized to represent t-SNARE present in a circular array. Studies using full length recombinant SNARE proteins and artificial lipid membranes demonstrated that t- and v-SNAREs located in opposing bilayers interact in a circular array to form conducting channels (Cho, et al., 2002d). Since similar circular structures are observed at the base of the pancreatic porosome complex, and SNAP-23 immunoreactivity is localized to the same site, these findings suggest the circular arrangement of proteins at the porosome base to be t-SNAREs.

The size and shape of the immunoisolated porosome complex has also been determined using both negative staining EM and AFM (Jeremic, et al., 2003). The morphology of immunoisolated porosomes obtained using EM and AFM, were similar, and found to be super-imposable (Jeremic, et al., 2003). The immunoisolated porosome complex has also been both structurally and functionally reconstituted into liposomes and lipid bilayer membrane (Cho, et al., 2004; Jeremic, et al., 2003). Transmission electron micrographs of pancreatic porosomes reconstituted into liposomes, exhibit a 150–200 nm cup-shaped basket-like morphology, similar to what is observed in its native state when co-isolated with ZGs.

In the past decade, a number of studies demonstrate the involvement of cytoskeletal proteins in cell secretion, some implicating a direct interaction of cytoskeleton protein with SNAREs (Bennett 1990; Faigle, et al., 2000; Goodson, et al., 1997; Nakano, et al., 2001; Ohyma, et al., 2001; Cho, et al., 2005b). Furthermore, actin

www.manaraa.com

and microtubule-based cytoskeleton has been implicated in intracellular vesicle traffic. Fodrin, which was previously implicated in exocytosis, has also been shown to directly interact with SNAREs (Nakano, et al., 2001). Studies demonstrate α-fodrin to regulate exocytosis via its interaction with t-SNARE syntaxin family of proteins. The C-terminal region of syntaxin is known to interact with α-fodrin, a major component of the submembranous cytoskeleton. Similarly, vimentin filaments interact with SNAP23/25 and hence are able to control the availability of free SNAP23/25 for assembly of the t-/v-SNARE complex (Faigle, et al., 2000). All these findings suggested that vimentin, α-fodrin, actin, and SNAREs may be part of the porosome complex. Additional proteins such as v-SNARE (VAMP or synaptobrevin), synaptophysin and myosin, may associate when the porosome establishes continuity with the secretory vesicle membrane. The globular tail domain of myosin V contains a binding site for VAMP, which is bound in a calcium independent manner (Ohyma, et al., 2001). Further interaction of myosin V with syntaxin had been shown to require both calcium and calmodulin. It had also been suggested that VAMP, may act as a myosin V receptor on secretory vesicles, and regulate formation of the SNARE complex (Nakano, et al., 2001). Interaction of VAMP with synaptophysin and myosin V had also been reported (Ohyma, et al., 2001).

In agreement with these earlier findings, our studies (Cho, et al., 2004; Jena, et al., 2003) demonstrate the association of SNAP-23, syntaxin 2, cytoskeletal proteins actin, α-fodrin, and vimentin, and calcium channels β3 and α1c, together with the SNARE regulatory protein NSF, in the porosome complex (Cho, et al., 2004; Jena, et al., 2003; Jeremic, et al., 2003). Additionally, chloride ion channels ClC2 and ClC3 were also identified as part of the porosome complex (Cho, et al., 2004; Jena, et al., 2003; Jeremic, et al., 2003). Isoforms of the various other proteins identified in the

www.manaraa.com

porosome complex, have also been demonstrated using 2D-BAC gels electrophoresis (Jeremic, et al., 2003). Three isoforms each of the calcium ion channel and vimentin were found in porosomes (Jeremic, et al., 2003). Using yeast two-hybrid analysis, recent studies confirm the presence and interaction of some of these proteins with t-SNAREs within the porosome complex (Cho, et al., 2005b).

Concomitant electrophysiological studies support AFM findings regarding porosome function. To test the functionality of the isolated porosome complex, purified porosomes obtained from exocrine pancreas or neurons were subjected to reconstitution in lipid membrane of the electrophysiological setup (EPC9), and challenged with isolated ZGs or synaptic vesicles. Electrical activity of the reconstituted membrane as well as the transport of vesicular contents from the *cis* to the *trans* compartments of the bilayer chambers was monitored. Results from these experiments demonstrate that the lipid membrane-reconstituted porosomes, are indeed functional (Cho, et al., 2004; Jeremic, et al., 2003), since in the presence of calcium, isolated secretory vesicles dock and fuse to transfer intravesicular contents from the cis to the trans compartment of the bilayer chamber. ZGs fused with the porosome-reconstituted bilayer as demonstrated by an increase in capacitance and conductance, and a time-dependent transport of the ZG enzyme, amylase, from *cis* to the *trans* compartment of the bilayer chamber (Figure 6A & B) (Jeremic, et al., 2003; Jena 2007). Amylase was detected using immunoblot analysis of the buffer in the *cis* and *trans* chambers, using immunoblot analysis (Jeremic, et al., 2003; Jena 2007). As observed in immunoblot assays of isolated porosomes, chloride channel activity is also present in the reconstituted porosome complex. Furthermore, the chloride channel inhibitor DIDS, was found to inhibit current activity through the porosome-reconstituted bilayer (Figure

www.manaraa.com

6C), demonstrating a requirement of the porosome-associated chloride channel activity

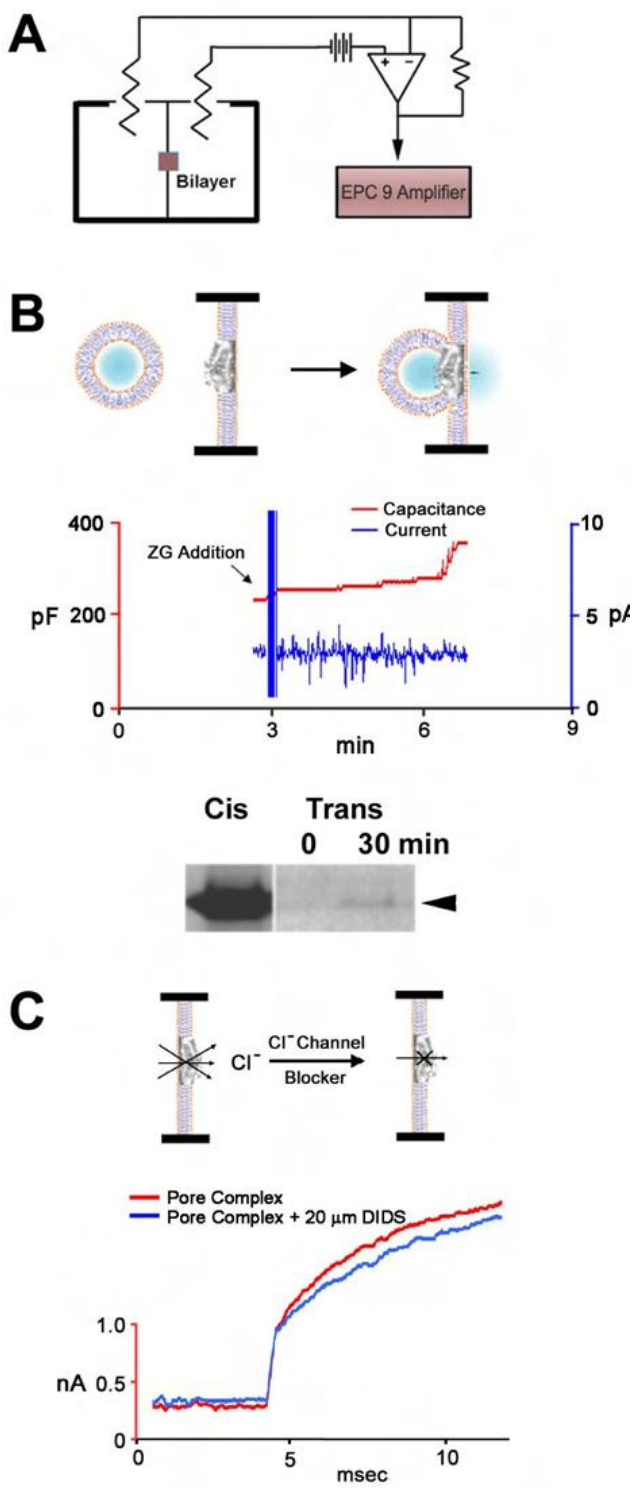

Figure 6. (A) Drawing of electrophysiological set up for lipid bilayer experiments. (B) ZG fuse to porosome reconstituted bilayer as show by increases in capacitance and

www.manaraa.com

appearance of amylase in trans side medium. (C) The addition of the anion channel blocker DIDS to the reaction buffer inhibited the fusion of ZGs to porosomes. (Jeremic et al., 2003a)

in porosome function. Similarly, the structure and biochemical composition of the neuronal porosome, and the docking and fusion of synaptic vesicles at the neuronal porosome complex has also been elucidated (Figure 7) (Cho, et al., 2004; Cho, et al.,

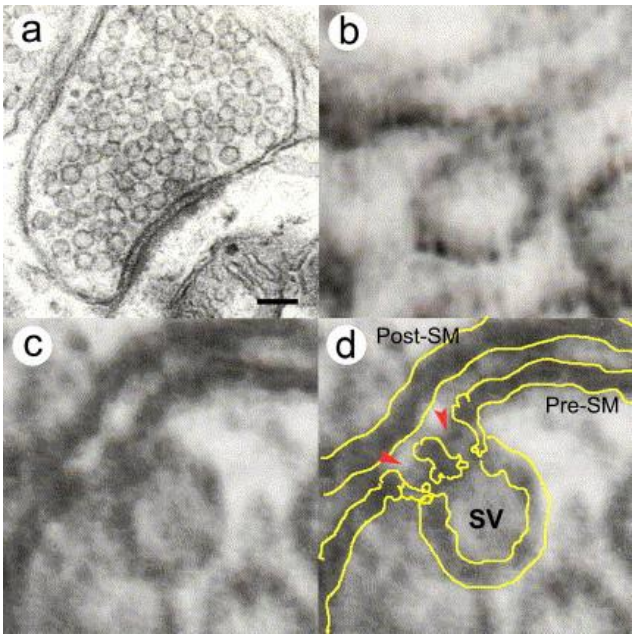

Figure 7. Neuronal fusion pore. (A) Electron micrograph of isolated synaptosome containing a large number of synaptic vesicles. Bar = 100nm (B-D) Higher magnification of a single synaptic vesicle docked to the plasma membrane at the porsome. (Cho et al., 2004)

2007). In summary, these studies demonstrate porosomes to be permanent supramolecular lipoprotein structures at the cell plasma membrane, where membrane-bound secretory vesicles transiently dock and fuse to release intravesicular contents to the outside. Porosomes are therefore the universal secretory machinery in cells (Jena 2007; Jena 2005; Jena 2004).

www.manaraa.com

SNARE Proteins

Soluble NSF attachment protein receptors (SNAREs) are a family of proteins, which are involved in membrane trafficking and secretory processes (Weber et al., 1998). At the plasma membrane, target SNAREs (or t-SNAREs) are comprised of the proteins syntaxin and SNAP (synaptosome associated protein), both which differ in isoform depending on cell type. Syntaxin-2 is mainly found in pancreatic acinar cells (Hansen et al., 1999) while syntaxin-1 (A and B) is localized to neuronal cells (Aguado et al., 1999). SNAP-25 is present almost exclusively in the brain in contrast to SNAP-23, which is widely distributed in many tissues, including pancreas (Ravichandran et al., 1996). t-SNAREs are present at the base of the porosome, as confirmed by AFM studies (Jeremic et al., 2003).

The structure and arrangement of SNAREs associated with lipid bilayers were first determined using AFM (Cho et al., 2002d), almost a decade ago. Electrophysiological measurements of membrane conductance and capacitance enabled the determination of fusion of v-SNARE-reconstituted liposomes with t-SNARE-reconstituted membrane. Results from these studies demonstrated that t-SNAREs and v-SNARE when present in opposing membrane interact and assemble in a circular array, and in presence of calcium, form conducting channels (Cho et al., 2002d). The interaction of t-/v-SNARE proteins to form such conducting channels is strictly dependent on the presence of t-SNAREs and v-SNARE in opposing membranes. Simple addition of purified recombinant v-SNARE to a t-SNARE-reconstituted lipid membrane, fails to form the SNARE ring complex, and is without influence on the electrical properties of the membrane (Cho et al., 2002d). However when v-SNARE

www.manaraa.com

vesicles are added to t-SNARE reconstituted membrane, SNAREs assemble in a ring conformation, and in the presence of calcium, establish continuity between the opposing membrane (Figure 8) (Jeremic et al., 2004). The establishment of continuity between

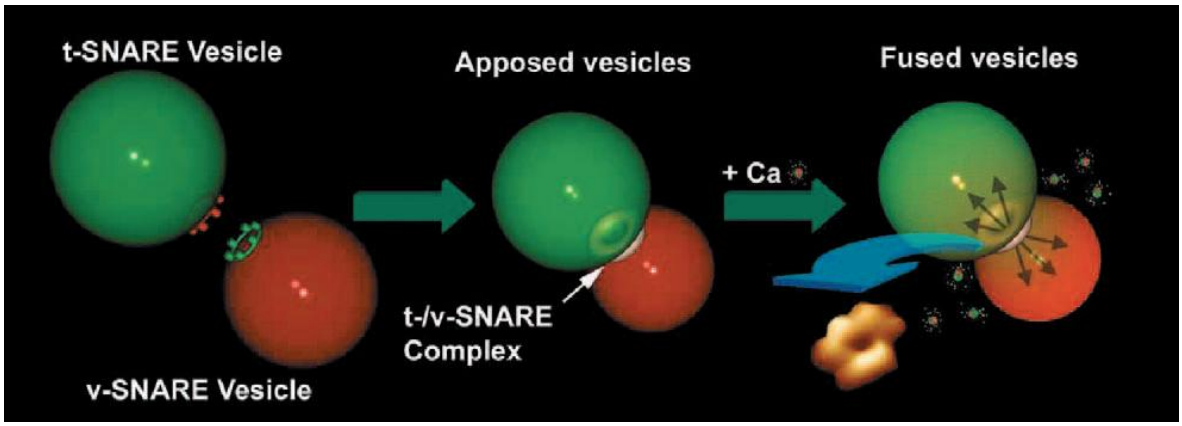

Figure 8. Illustration demonstrating t-/v-SNARE complex formation between t- and v-SNARE reconstituted liposomes. In the presence of calcium, lipid membrane continuity is established and a circular pore or channel is produced. (Jeremic et al., 2004)

the opposing t-SNARE and v-SNARE reconstituted bilayers, is reflected in the increase in membrane capacitance and conductance. These results confirm that t- and v-SNAREs are required to reside in opposing membrane, similar to their presence in cells, to allow appropriate t-/v-SNARE interactions leading to membrane fusion (Cho et al., 2002d; Cho et al., 2005a).

Membrane curvature dictates the size of the SNARE ring complex. When t-SNARE- and v-SNARE-reconstituted proteoliposomes of different diameters were examined, they gave rise to different size t-/v-SNARE ring complexes (Cho et al., 2005). It was demonstrated that the larger the vesicle, the greater the diameter of the SNARE ring complex. The experimental data fit well with the high correlation coefficient, R^2=0.9725 between vesicle diameter and SNARE-complex size. These studies verify

www.manaraa.com

that SNARE interaction is synonymous despite a difference in size of the liposome to which they are found; however, the size of the complex is augmented in relation to the size of the vesicle in a linear fashion. These results also indicate that, as in vivo, vesicle size ranges (30-50nm in diameter in neurons to 100's of nm in diameter in zymogen granules) do not disrupt the function of these proteins.

Furthermore, the proper folding of the SNARE proteins requires the presence of lipid membrane, as determined by AFM and circular dichroism (CD) spectroscopy investigations. Resolution of the crystal structure of truncated non-membraneous SNARE complex reveals that in its core domain, it is comprised of a bundle of four SNARE motifs of intertwined α-helical structures (Figure 9) (Sutton et al., 1998). Upon

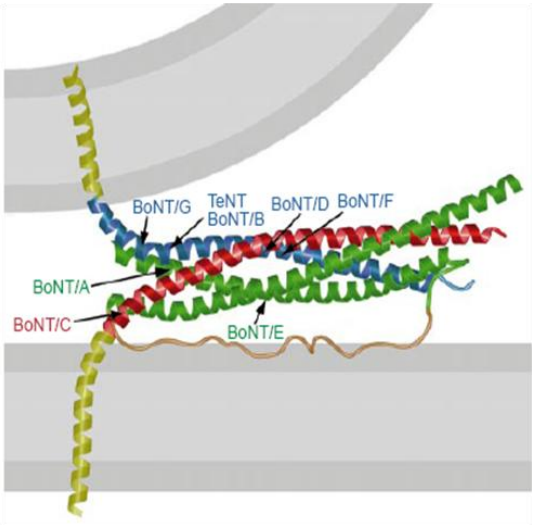

Figure 9. Schematic depiction of the crystal structure of truncated non-membrane associated SNARE complex. Syntaxin 1A shown in red, synaptobrevin-II shown in blue, their transmembrane domains shown in yellow, and the loop connecting the Sn1 and Sn2 fragments shown in green. (Sutton et al., 1998)

investigation of the secondary structure of the t- and v-SNAREs using CD spectroscopy, both in suspension and reconstituted into liposomes, results indicate decreased folding of both SNAREs when membrane associated. This finding can be attributed to protein

www.manaraa.com

insertion into the lipid membrane due to the association of hydrophobic protein domains with the phospholipids. When t- and v-SNARE reconstituted liposomes are incubated simultaneously, SNARE complexes form; however, there is no increase in secondary structure. Addition of NSF and ATP to SNARE complexes in suspension and in membrane dissociate with almost complete loss of α-helices. This finding supports previous studies which indicate that NSF and ATP are the minimal requirements for complex disassembly. In agreement with AFM images depicting t-/v-SNARE complexes forming globular-like structures when non-membrane associated, CD spectroscopic data on the secondary nature of these proteins demonstrates that proper folding requires lipid (Cook et al., 2008).

In contrast to the spontaneous association of t- and v-SNAREs in opposing membranes, dissociation of the complex requires an input of energy (ATP) and the presence of NSF, a soluble ATPase protein (Jeremic et al., 2006; Littleton et al., 2001). Light scattering profiles in real time reveal the requirement of both NSF and ATP to dissociate t-/v-SNARE vesicles. These findings were reinforced by immunoblot, CD spectroscopic, and AFM analyses of t-/v-SNARE associated vesicles with or without NSF and ATP. If either NSF or ATP is not present in the reaction sample, t-/v-SNARE complexes remain associated (Jeremic et al., 2006; Cook et al., 2008).

SNARE-induced Membrane Fusion

As previously mentioned, SNARE proteins interact to pull opposing lipid membranes into closer proximity; however, this mechanism itself is not responsible for the establishment of lipid bilayer continuity during the formation of a channel. The dilemma of establishing a channel between the vesicle and cell plasma membrane lies in the natural repulsion between the polar phospholipid head groups. Consequently, a

www.manaraa.com

mechanism that would allow the lipids to associate with one another, overcoming the repulsive forces of the negatively charged lipid head groups is necessary to mediate membrane fusion and subsequent cell secretion.

It has long been understood that calcium is a mediator of vesicle fusion in neurotransmission. Cumulating evidence such as the finding that calcium channels and calcium binding proteins (for example synaptotagmin) are associated with the SNARE complex, also support this molecule's role in cell secretion (Jeremic et al., 2003). Light scattering experiments using t- and v-SNARE reconstituted liposomes indicate that calcium (Ca^{2+}) in the sample buffer is required for fusion of the opposing vesicles. X-ray diffraction analysis of hydrated Ca^{2+} demonstrates that the ion with its first layer or shell of hydration consists of six water molecules in an octahedral arrangement at a size of 6Å. The proposed mechanism of calcium mediated fusion postulates that once the hydrated calcium interacts with the negatively charged phospholipid head groups on the opposing membranes, water is discharged locally and phospholipids are destabilized, which enables them to mix and fuse. The resulting dehydrated calcium ion has an ionic radius of approximately 2.56Å (Figure 10B, C, D). SNAREs bring opposing membranes to within a distance of 2.8 to 3Å, which allows the dehydrated calcium ion to fit and bridge the opposing bilayers (Figure 10B, C, D). These results agree both spatially and with the findings that calcium must be present in the cellular medium before SNARE interaction takes place (Jeremic et al., 2004).

www.manaraa.com

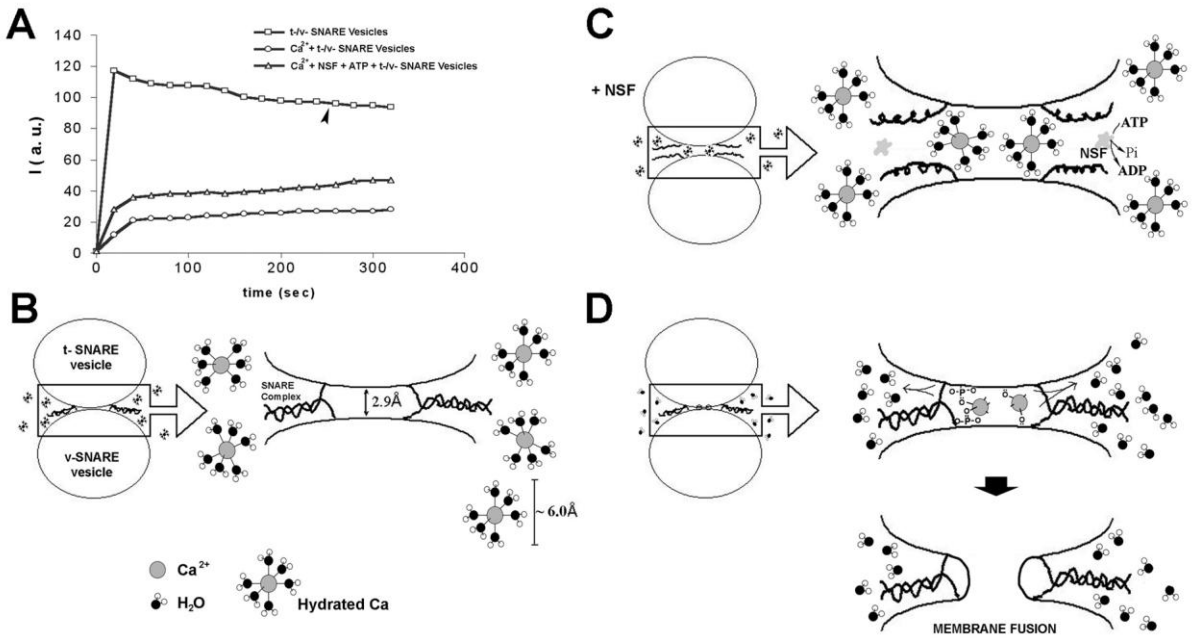

Figure 10. Light scattering profiles of SNARE-associated vesicle interactions. A,B. Addition of t-SNARE and v-SNARE vesicles in calcium-free buffer lead to a significant increase in light scattering. Subsequent addition of 5 mM Ca^{2+} (marked by the arrowhead) does not have any significant effect on light scattering (□). A,C. In the presence of NSF-ATP (1 µg/ml) in the assay buffer containing 5 mM Ca^{2+}, significantly inhibited vesicle aggregation and fusion (Δ). Pi denotes inorganic phosphate. A,D. When the assay buffer was supplemented with 5 mM Ca^{2+}, prior to the addition of t- and v-SNARE vesicles, it led to a 4-fold decrease in light scattering intensity due to Ca^{2+}-induced aggregation and fusion of t-/v-SNARE-apposed vesicles (O). Light scattering profiles shown are representatives of 4 separate experiments. (Jeremic et al., 2004)

Expulsion of Intravesicular Contents

Once membrane continuity is established between compartments (membrane-bound secretory vesicles at the porosome base), vesicular contents must be released to the outside of the cell. Kinetically, simple diffusion out of the vesicle into the extracellular medium is not favorable, especially when considering that neurotransmission occurs on a sub-millisecond time scale (Sabatini & Regehr 1996). Accordingly, an inherent system by which cell secretion can occur quickly had to be established. The cell overcomes this predicament by exploiting an intravesicular

www.manaraa.com

electrochemical gradient, which allows for the entry of water into its vesicles and subsequent expulsion of vesicular cargo (Shin et al., 2010).

Vesicle swelling is a requirement for content expulsion during cell secretion (Kelly et al., 2004). Isolated live pancreatic acinar cells in near physiological buffer when imaged using AFM at high force (200-300 pN), demonstrate the size and shape of the ZGs lying immediately below the apical plasma membrane of the cell. Within 2.5 minutes of exposure to a physiological secretory stimulus, the majority of ZGs within cells swell, followed by a decrease in ZG size by the time secretion is complete. These studies reveal for the first time in live cells, intracellular swelling of secretory vesicles following stimulation of cell secretion and their deflation following partial discharge of vesicular contents. No loss of secretory vesicles is observed throughout the experiment. Measurements of intracellular ZG size further reveal that individual vesicles swell differently from one another, following a secretory stimulus. For example, the ZG marked by the red arrowhead swelled to show a 23-25% increase in diameter, in contrast to the green arrowhead-marked ZG, which increased by only 10-11% (Figure 2). This differential swelling among ZGs within the same cell, may explain why following stimulation of secretion, some intracellular ZGs demonstrate the presence of less vesicular content than others, and hence have discharged more of their contents. To determine precisely the role of swelling in vesicle-plasma membrane fusion and in the expulsion of intravesicular contents, an electrophysiological ZG-reconstituted lipid bilayer fusion assay has been employed. The ZGs used in the bilayer fusion assays were characterized for their purity and their ability to respond to a swelling stimulus. As previously reported (Jena et al., 1997; Cho et al., 2002c), exposure of isolated ZGs to GTP results in ZG swelling. Similar to what is observed in live acinar cells, each

www.manaraa.com

isolated ZG responds differently to the same swelling stimulus. This differential response of isolated ZGs to GTP has been further assessed by measuring changes in the volume of isolated ZGs of different sizes. ZGs in the exocrine pancreas range in size from 0.2 to 1.3 µm in diameter (Jena et al., 1997), not all ZGs are found to swell following a GTP challenge (Kelly et al., 2004). In most ZGs, volume increases are between 5-20%, however, larger increases of up to 45% are observed only in vesicles ranging from 250 nm to 750 nm in diameter. In the electrophysiological bilayer fusion assay, immunoisolated porosome complex from the exocrine pancreas, are functionally reconstituted into the lipid membrane of the bilayer apparatus, where membrane conductance and capacitance can be continually monitored. Reconstitution of the porosome into the lipid membrane results in a small increase in capacitance, possibly due to the increase in membrane surface area. Isolated ZGs when added to the *cis* compartment of the bilayer chamber, fuse at the porosome-reconstituted lipid membrane and is detected as a step increase in membrane capacitance. Even after 15 min of ZG addition to the *cis* compartment of the bilayer chamber, little or no release of the intra-vesicular enzyme α-amylase is detected in the *trans* compartment of the bilayer chamber. On the contrary, exposure of ZGs to 20 µM GTP, induced swelling and results both in the potentiation of fusion as well as a robust expulsion of α-amylase into the *trans* compartment of the bilayer chamber observed in immunoblot assays. These studies demonstrate that during cell secretion, secretory vesicle swelling is required for the efficient expulsion of intravesicular contents. This mechanism of vesicular expulsion during cell secretion may explain why partially empty vesicles are generated in cells following secretion. The presence of empty secretory vesicles could result from multiple rounds of fusion-swelling-expulsion cycles a vesicle may undergo

www.manaraa.com

during the secretory process, reflecting on the precise and regulated nature of cell secretion.

Previous studies have shown that zymogen granules swell (or increase in size) in response to GTP, implicating the involvement of a G-protein coupled mediated signaling pathway in vesicles, specifically $G_{\alpha i3}$ in these organelles. It has also been shown that water channels, known as aquaporins (AQPs) induce rapid volume changes in vesicles (Yasui et al., 1999). Appropriately, the presence of aquaporins in vesicles was demonstrated in multiple cells types: AQP1 in zymogen granules and AQP6 in synaptic vesicles (Cho et al., 2002c; Jeremic et al., 2005).

Immunoblot analysis of pancreatic tissue fractions depicts an enrichment of AQP1 in zymogen granule membranes in greater proportion than any other tissue fraction. Immunofluorescently labeled AQP1 observed under a confocal microscope shows preferential localization of this protein at the apical end of pancreatic acinar cells, as confirmed by electron microscope images depicting AQP1 in zymogen granule membranes. These findings were corroborated with immuno AFM imaging of AQP1 in zymogen granules in concert with GTP induced ZG swelling imaging via AFM. To further demonstrate AQP1's involvement in ZG swelling, administration of a water channel blocker (mercury chloride or $HgCl_2$), inhibited (but did not abolish) GTP induced ZG expansion (Cho et al., 2002c). These studies provide evidence indicating that AQP1 is a regulator and found upstream of the GTP induced ZG swelling pathway, and therefore, modulates cell secretion.

Successive research has elucidated the role of water channels (AQP6) in synaptic vesicle swelling. In response to GTP and mastoparan (an amphipathic tetradecapeptide that selectively activates $G_{i/o}$ proteins), photon correlation

www.manaraa.com

spectroscopy (PCS) results report approximately 100% increases in synaptic vesicle size. Additionally, inclusion of $HgCl_2$ into the reaction medium produced abrogated swelling. Through immunoblot analysis, it was determined that AQP1 and AQP6 (predominately) are found in synaptic vesicles (Jeremic et al., 2005).

Furthermore, synaptic vesicle membranes have also been shown to contain vH^+-ATPases (Stadler & Tsukita, 1984). Vesicle acidification through H^+ uptake via the vH^+-ATPase pump is a requirement for neurotransmitter transport into the organelle (Füldner & Stadler, 1982). Not only is neurotransmitter movement into synaptic vesicles modulated by vH^+-ATPases, these proton carriers have also been suggested to participate in neurotransmitter release (Morel et al., 2001).

Mastoparan has the ability to act as an activated beta-receptor by insertion and formation of an α-helical structure analogous to intracellular domains of G-protein coupled adrenergic receptors. Because of this property, it was postulated and determined that adrenoceptors and an endogenous β-adrenergic agonist exists at the synaptic vesicle membrane (Chen et al., 2010). Through western blot analysis and a series of swelling experiments, adrenergic receptors were shown to be present in synaptic vesicles and involved in the GTP mediated swelling pathway.

These in addition to many other investigations indicate that multiple proteins are involved in vesicle swelling. For example, potassium (K^+) and chloride (Cl^-) channels have been found in zymogen granule membranes and implicated in the expulsion process (Abu-Hamdah et al., 2004). Concurrently, the synergistic actions of all the components (which have yet to be determined) involved in the swelling process culminate in the rapid entry of water into the porosome-fused-vesicle, which creates a turgid pressure, causing intravesicular content expulsion out of the fusion pore and into

www.manaraa.com

the extracellular space (Kelly et al., 2004).

RESEARCH DESIGN AND METHODS

The investigations on cellular secretion mechanisms have shed insight and altered the commonly accepted dogma of complete vesicle merger with the cell plasma membrane. Collectively, these studies reveal the dynamic yet elegant, and highly regulated nature of cell secretion; where membrane-bound secretory vesicles transiently dock and fuse at the base of plasma membrane-associated structures called porosomes, to expel vesicular contents from the cell. However, not all facets of this mode by which cells secrete have been fully elucidated. For example the molecular mechanism of membrane-associated SNARE assembly and disassembly required for fusion of secretory vesicles at the base of porosomes, or the molecular mechanism of secretory vesicle swelling required for the expulsion of intravesicular contents during cell secretion, remained to be determined. This is what I set out to determine in my studies.

The cell membrane has many functions ranging from acting as a semi-permeable barrier to its direct involvement in signal transduction, where membrane lipids are cleaved as in inflammatory pathways catalyzed by the enzyme phospholipase A2. Because of its wide range of properties, it is necessary for the cell membrane to remain both flexible (for example during fusion of vesicles with the plasma membrane in transport functions) yet durable (as a semi-permeable barrier). Previous studies have revealed that the lipid composition of cellular membranes is critical to normal functioning of the cell and that changes in lipid proportions in the plasma membrane can affect the function of that cell. Specifically, it has been shown that cholesterol interacts with a number of proteins within the porosome complex and regulates neurotransmitter

www.manaraa.com

release. Some of these proteins include calcium ion channels and VAMP (Zamir and Charlton 2006). It has also been established that t-SNAREs congregate in large cholesterol-dependent clusters at the plasmalemma and when cholesterol is depleted from these areas, it results in the dispersion of the t-SNARE proteins as well (Lang et al., 2001). A 2007 study by Cho and others demonstrated that the presence of cholesterol in the cell plasma membrane is required for the structural and functional integrity of the porosome. Interestingly, this study also found that depletion of cholesterol had no effect on the assembly of SNARE proteins during secretion.

Additionally, it has been confirmed that another membrane lipid, LPC, has effects on hormonal secretion (Han et al., 2003; Jougasaki 1992) and both cholesterol and LPC affect the membrane curvature of the cell. Cholesterol imparts a negative curvature to the cell membrane, causing it to become less curved (Wang et al., 2007). LPC on the other hand imparts a positive curvature, inducing the membrane to become more curved (Chernomordik 1996). Previous studies have demonstrated that the curvature of the membrane influences functions of the cell, such as secretion (McMahon & Gallop 2005). Therefore, it is apparent that both cholesterol and LPC influence secretory processes, yet their precise molecular interactions with secretory proteins were not understood.

Following SNARE-induced secretory vesicle docking and fusion at the porosome base, vesicle swelling leading to intravesicular pressure and expulsion of intravesicular contents occurs (Kelly et al., 2004). It has been determined that vesicle membranes contain a number of proteins which are involved in a G-protein mediated signaling cascade that leads to the opening of aquaporin channels within the vesicle membrane and entry of water to cause the vesicle to rapidly swell (Cho et al., 2002c; Jeremic et al.,

www.manaraa.com

2005). Previous studies have verified the presence of vH^+-ATPases within vesicle membranes and have elucidated their function to acidify the vesicle for neurotransmitter uptake into the organelle (Michaelson & Angel, 1980; Füldner & Stadler, 1982). It has also been established that vH^+-ATPases influence neurotransmitter secretion (Morel et al., 2001; Peters et al., 2001). Although a number of proteins have been implicated within the secretory process, the exact order and the influence of vH^+-ATPases on the signaling cascade within the vesicle membrane was not known.

Non structural lipid bilayer molecules such as cholesterol and LPC have been shown to influence cell secretion, yet their interactions with SNARE proteins have not been investigated. Although the dynamics of secretory vesicle swelling and content expulsion have been studied, certain details underlying the process remained to be fully elucidated. In view of this, the following research objectives were investigated:

Objective #1: Determine how membrane lipids, specifically cholesterol and LPC, influence the assembly and disassembly of membrane-associated SNARE complex.

Objective #2: Understanding the regulation of vesicle swelling by the vH^+-ATPase proton pump.

www.manaraa.com

CHAPTER 2

MEMBRANE LIPIDS INFLUENCE PROTEIN COMPLEX ASSEMBLY-DISASSEMBLY

INTRODUCTION

The process of cell secretion requires the interaction of SNARE proteins both at plasma and vesicle membranes. t-SNAREs (or target SNAREs) located at the cell plasma membrane are comprised of syntaxin and SNAP proteins. These target SNAREs associate with vesicle (or v-SNARE) proteins to pull the opposing bilayers into closer proximity. In the presence of calcium, continuity is established to form a channel or pore for expulsion of vesicular contents (Jeremic et al., 2004). A deeper understanding of the molecular mechanisms underlying SNARE complex formation requires an investigation of the structural changes that occur at the atomic level during SNARE assembly and disassembly.

As previously described, the crystal structure of the SNARE complex is comprised of an intertwined four α-helical bundle (Sutton et al., 1998). CD spectroscopic studies done in 2008 by Cook et al. reveal that SNARE folding is dependent on the presence of a lipid bilayer. SNAREs in membrane versus in suspension displayed significantly decreased α-helical character (or decreased folding). These findings should not come as a surprise since VAMP and syntaxin are both integral membrane proteins; therefore, their folding profiles are affected by the absence of a lipid bilayer. When in suspension, the hydrophobic regions self-associate to shield themselves from the aqueous medium. Comparison of t-SNAREs, t-/v-SNAREs, and t-/v-SNAREs with NSF, both in suspension and in membrane, demonstrates high α-helical content. Interestingly, this study also reported an almost complete elimination of α-helices upon the addition of ATP to the t-/v-SNARE-NSF complex, providing support

www.manaraa.com

for earlier studies on SNARE-NSF complex dissociation in the presence of ATP (Jeremic et al., 2006).

Elaborating on the former study by Cook et al., although lipid is required for proper SNARE folding, membrane lipid composition varies between cell types (Spektor & Yorek 1985). Non-structural membrane lipids, cholesterol and LPC, are known to influence secretory processes in the cell (Cho et al., 2007; Han et al., 2003). Cholesterol is a critical component of cellular membranes. It has also been implicated to participate in neurotransmitter release (Zamir & Charlton, 2006). It is because of these characteristics of cholesterol that peaked interest to examine whether this molecule had any influence on the porosome and process of cell secretion. In a 2007 study by Cho et al., isolated synaptic membrane preparations when depleted of cholesterol, displayed a decrease in porosome integrity but had no effect on t-/v-SNARE complex assembly.

Additionally, both cholesterol and LPC influence cell membrane curvature. Cholesterol imparts a negative curvature to the cell membrane (Wang et al., 2007). It causes the membrane to curve away from the cytoplasm or in essence, flatten the membrane. Conversely, LPC imparts a positive curvature to the cell membrane (Chernomordik 1996), or more simply, causes the membrane to curve towards the cell cytoplasm. Since curvature itself is also known to modify cellular processes, including secretion, mobility and trafficking (McMahon & Gallop 2005), investigation into the molecular mechanisms underlying the interactions between these membrane lipids with the SNARE complex is pertinent to our understanding of process of cell secretion.

Experimental Overview

Full length recombinant SNARE proteins expressed in *E. coli* were reconstituted

www.manaraa.com

into liposomes (synthetic vesicles) with and without cholesterol and LPC. Since vesicle size influences membrane curvature, uniform samples of 50 nm in diameter vesicles were used for this study. Samples were observed using CD spectroscopy to determine the secondary folding profiles of v-SNAREs, t-SNAREs, t-/v-SNAREs, t-/v-SNAREs + NSF, and t-/v-SNAREs + NSF and ATP. AFM images of t- and v-SNAREs and their complexes were also obtained to confirm CD spectroscopic results.

Detailed Materials and Methods

Protein Purification N-terminal 6xHis-tag constructs for SNAP-25 and NSF, C-terminal 6xHis-tag constructs for Syntaxin 1A and VAMP2 were generated. All four proteins were expressed with 6xHis at full length in *E. coli (BL21DE3)* and isolated by Ni-NTA (nickel-nitrilotriacetic acid) affinity chromatography (Qiagen, Valencia, CA). Protein concentration was determined by BCA assay.

Preparation of Proteoliposomes All lipids were obtained from Avanti Polar Lipids (Alabaster, AL). For the control group, a 5 mM lipid stock solution was prepared by mixing lipid solution in chloroform-DOPC (1,2-dioleoyl phosphatidylcholine): DOPS (1,2-dioleoyl phosphatidylserine) in 70:30 mol/mol ratios in glass test tubes. For the cholesterol group, a 5 mM lipid stock solution was prepared by mixing lipid solution in chloroform-DOPC (1,2-dioleoyl phosphatidylcholine): DOPS (1,2-dioleoyl phosphatidylserine): cholesterol in 63:27:10 mol/mol/mol ratios in glass test tubes. For the LPC group, 5 mM lipid stock solution was prepared by mixing lipid solution in chloroform-DOPC (1,2-dioleoyl phosphatidylcholine): DOPS (1,2-dioleoyl phosphatidylserine): LPC (L-α-Lysophosphatidlycholine) in 63:27:10 mol/mol/mol ratios in glass test tubes. The lipid mixture was dried under gentle stream of nitrogen and resuspended in sodium phosphate buffer. Lipids were suspended in 5mM sodium

www.manaraa.com

phosphate buffer, pH 7.5, by vortexing for 5 min at room temperature. Unilamellar vesicles were formed following sonication for 2 min, followed by a 50 nm pore size extruder. Typically, vesicles ranging in size from 80-100 nm in diameter were obtained as assessed by AFM and photon correlation spectroscopy. Two sets of proteoliposomes were prepared by gently mixing either t-SNARE complex (Syntaxin-1/SNAP-25; final concentration 25 µM) or VAMP2-His_6 (final concentration 25 µM) with liposomes (Cho et al., 2002d; Jeremic et al., 2004) followed by three freeze/thaw cycles to enhance protein reconstitution at the vesicles membrane.

Atomic force microscopy on liposomes Atomic force microscopy was performed on liposomes placed on mica surface in buffer. Liposomes were imaged using the Nanoscope IIIa AFM from Digital Instruments. (Santa Barbara, CA). Images were obtained in the "tapping" mode in fluid, using silicon nitride tips with a spring constant of 0.38 $N.m^{-1}$, and an imaging force of <200 pN. Images were obtained at line frequencies of 2 Hz, with 512 lines per image, and constant image gains. Topographical dimensions of the lipid vesicles were analyzed using the software nanoscope IIIa4.43r8, supplied by Digital Instruments.

Circular Dichroism (CD) Spectroscopy Overall secondary structural content of both soluble and membrane associated SNARE complexes were determined by CD spectroscopy using an Olis DSM 17 spectrometer. Data was collected at 20^{o}C with a 0.01 cm pathlength quartz cuvette (Helma); spectra were collected over a wavelength range of 190 – 260 nm using a1 nm step spacing. Five scans were averaged per sample for enhanced signal to noise, and data were collected on duplicate independent samples to ensure reproducibility. Liposome, liposome+cholesterol, and liposome+LPC associated protein and protein complex samples were analyzed for the following

www.manaraa.com

samples: v-SNARE, t-SNARE, v-SNARE + t-SNARE, v-SNARE + t-SNARE + N-ethylmaleimide Sensitive Factor (NSF), v-SNARE + t-SNARE + NSF + 2.5mM ATP. All samples had final protein concentrations of 25µM in 5mM NaPi buffer pH 7.5 and were baseline subtracted to remove buffer (or liposome in buffer) signal. Data was analyzed using the supplied GlobalWorks software (Olis), which incorporates a smoothing function (Gorry 2002), and fit using the CONTINLL algorithm (Provencher & Glockner 1981).

Results and Discussion

AFM results indicate a significant difference between SNARE ring complexes formed from reconstituted liposomes with cholesterol versus LPC, approximately 6.89 and 7.746 nm respectively (Figure 11). CD spectroscopic data also indicate profound differences in SNARE complexes between cholesterol and LPC groups. Both groups indicate high α-helical content in t-SNAREs, t-/v-SNAREs, and t-/v-SNAREs + NSF. These results were consistent with the previous study done by Cook et al., 2008; however in the present study, upon the addition of ATP to t-/v-SNARE complexes with NSF, cholesterol groups displayed a complete abolishment of α-helices, while t-/v-SNARE complexes from LPC groups did not show a change in the presence of NSF and ATP (Table 1). These changes were also apparent in CD graphical analyses demonstrating alterations in wavelength peaks at 208 and 222 nm, which are characteristic of α-helical secondary structure (Figure 12).

CD spectra of membrane-associated v-SNARE displayed little signal (Figure 12Ai, Bi), as was consistent with previous studies (Cook et al., 2008); yet cholesterol groups showed high α-helical content in contrast to the low content seen in LPC groups (Table 1). These findings could be attributed to the limitations of the spectrometer and

www.manaraa.com

of GlobalWorks software (Olis) in analyzing and fitting data with such weak signals. Nevertheless, v-SNARE data was run to ensure no inappropriate protein signals were present, which could negatively impact the data obtained from t-/v-SNARE complexes.

In cholesterol and LPC groups, t-SNARE and t-/v-SNARE data obtained from this study correlated with the previous study by Cook et al., 2008. Surprisingly, significant differences were found when NSF and ATP were added to t-/v-SNARE complexes in cholesterol and LPC groups. In LPC groups, t-/v-SNARE complex disassembly was inhibited, as was demonstrated by the lack of change in α-helical content in the presence of NSF and ATP (Table 1). Furthermore, addition of NSF and ATP to t-/v-SNARE complexes in cholesterol groups did not influence β-sheet structure; however, in LPC groups, β-sheet structure was nearly completely abolished (Table 1). These results are consistent with studies indicating that LPC inhibits membrane fusion (Mitter et al., 2003). These findings indicate the existence of a direct lipid-protein relationship that modulates the function of SNARE proteins. Modifying membrane lipid diversity could influence the degree and rate of membrane fusion and membrane-directed SNARE complex assembly-disassembly. Cells with higher distribution of cholesterol would promote membrane fusion while cells with greater concentration of LPC would facilitate initial secretory event longevity by inhibiting complex disassembly.

www.manaraa.com

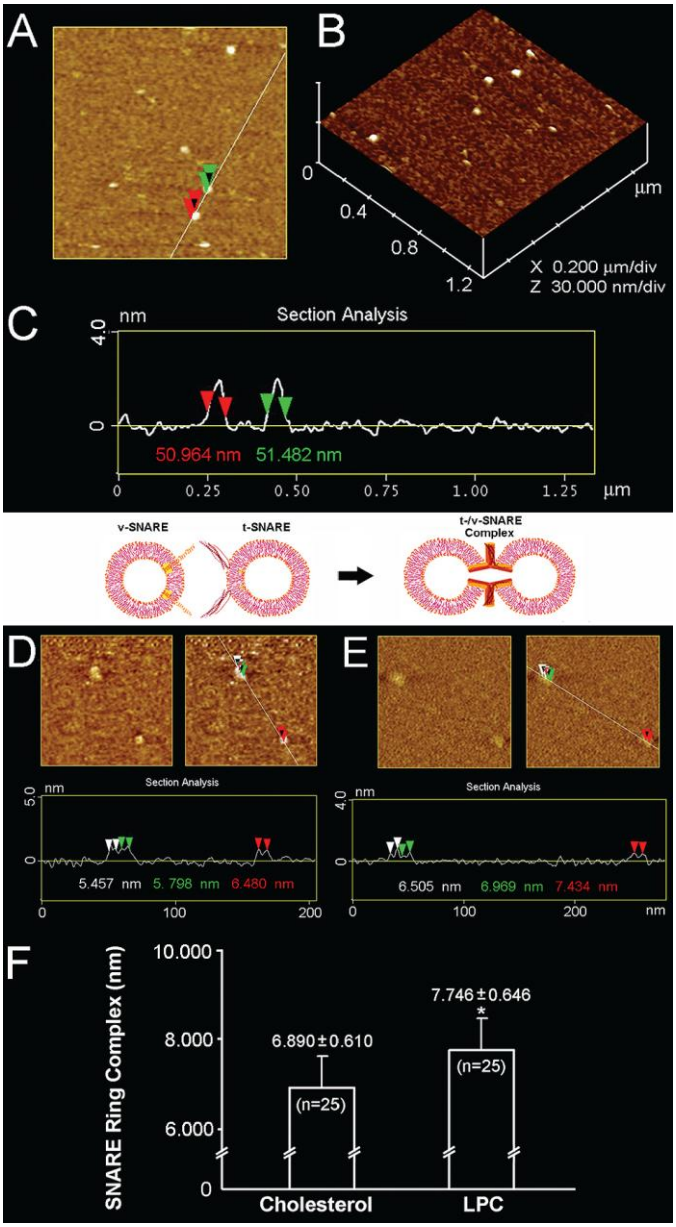

Figure 11. Representative AFM micrographs of ~50 nm diameter liposomes and the t-/v-SNARE ring complexes formed when such cholesterol- or LPC containing t-SNARE and v-SNARE proteoliposomes meet. (A-C) 50-53 nm diameter cholesterol-containing liposomes. Similarly sized LPC containing vesicles were prepared and observed using AFM (data not shown). (D, F) 6.89 ± 0.61 nm t-/v-SNARE ring complexes formed when ~50 nm diameter t-SNARE-cholesterol liposomes interact with 50 nm v-SNARE-cholesterol vesicles. (E, F) Similar 7.746 ± 0.646 nm t-/v-SNARE ring complexes formed by replacing cholesterol with LPC. * indicates $p < 0.001$. (Shin et al., 2010)

www.manaraa.com

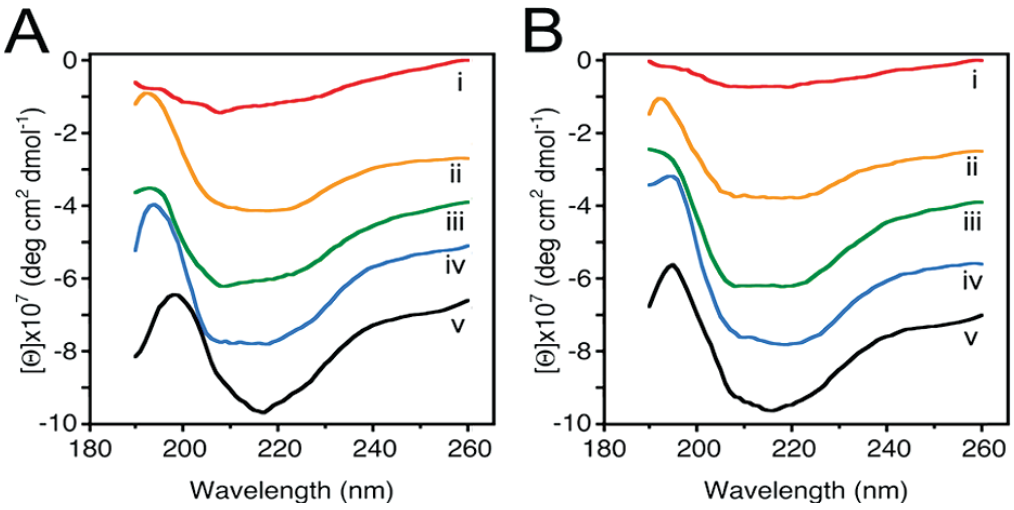

Figure 12. CD data reflecting structural changes to SNAREs associated with liposomes containing (A) cholesterol and (B) LPC. Structural changes following the assembly and NSF-ATP-induced disassembly of the t-/v-SNARE complex are further shown: (i) v-SNAREs; (ii) t-SNAREs; (iii) t-/v-SNARE complex; (iv) t-/v-SNARE complex + NSF; and (v) t-/v-SNARE + NSF + 2.5 mM ATP. CD spectra were recorded at 25 ºC in 5 mM sodium phosphate buffer (pH 7.5) at a protein concentration of 25 µM. In each experiment, scans were averaged per sample for enhanced signal-to-noise, and data were acquired on duplicate independent samples to ensure reproducibility. The decrease in α-helicity in the cholesterol groups as opposed to the LPC groups following exposure of the t-/v-SNARE complex to NSF-ATP should be noted (Table1). (Shin et al., 2010)

Table 1. Secondary Structural Fit Parameters of SNARE Complex Formation and Dissociation[a]

	cholesterol group					LPC group				
	liposome + cholesterol (100*f*)					liposome + LPC (100*f*)				
protein[b]	α	β	O	U	fit[c]	α	β	O	U	fit[c]
v-SNARE	21	28	0	51	0.11	0	23	32	44	0.38
t-SNARE	20	18	11	51	0.17	21	22	0	57	0.22
t-/v-SNARE	27	29	0	45	0.10	26	20	0	55	0.22
t-/v-SNARE + NSF	18	2	6	75	0.26	22	17	3	58	0.25
t-/v-SNARE + NSF + ATP	0	21	40	39	0.20	20	3	0	76	0.10

[a] Abbreviations used: *f*, fraction of residues is a given conformational class; α, α-helix; β, β-sheet; O, other (sum of turns, distorted helix, distorted sheet); U, unordered. [b] Protein constructs: v-SNARE (VAMP2); t-SNAREs (SNAP-25 + syntaxin 1A); NSF, *N*-ethylmaleimide-sensitive factor; ATP, adenosine triphosphate. [c] Fit: goodness-of-fit parameter expressed as normalized spectral fit standard deviation (nm).

www.manaraa.com

CHAPTER 3

LYSOPHOSPHATIDYLCHOLINE REGULATES MEMBRANE PROTEIN COMPLEX DISASSEMBLY

INTRODUCTION

Recent findings have shown that structural membrane lipids influence membrane fusion via interactions with SNAREs and SNARE chaperones (Mima & Wickner, 2009); however, the importance of non structural membrane lipids (such as LPC and cholesterol) on secretion is only partially understood. The previous investigation by Shin et al. in 2010 revealed that full length recombinant SNAREs reconstituted in lipid membrane (synthetic vesicles, also known as liposomes) will associate to form SNARE complexes that dissociate in the presence of NSF and ATP, as demonstrated by a change in α-helical content. Additionally, membranes containing LPC generate larger SNARE ring complexes, where the α-helical component of the complex is little affected by NSF-ATP (Shin et al., 2010). In contrast, cholesterol-containing membranes produce smaller SNARE ring complexes that readily disassemble in the presence of NSF-ATP (Shin et al., 2010). These findings suggest that in the presence of LPC, subsequent rounds of secretion are inhibited and the initial contact between secretory vesicle and plasma membrane is maintained due to the inability of NSF-ATP to disassemble the SNARE complex (Shin et al., 2010). Although these studies have given us insight into the molecular dynamics of SNARE assembly and disassembly, the interaction between SNARE proteins and membrane lipids is incompletely understood.

A recent review by McIntosh and Simon in 2006 discussed the influence of membrane lipid composition on the distribution, function and organization of membrane proteins. This paper analyzed recent research findings to show that both the lipid

www.manaraa.com

environment and the individual interactions of lipid molecules with membrane proteins can alter protein properties. For example, membrane lipid composition alters the electrostatic charge of the membrane. The charge of the membrane can then determine the concentration of peptides with a net positive or negative charge that will accumulate in such a membrane. Furthermore, the lipid composition of the cell membrane will influence the binding of proteins and that the deformation of the membrane is constrained by energy barriers, which have to be overcome in order for protein interactions to occur. In agreement with these findings, another review article by Zimmerberg and Chernomordik, published in 2005, demonstrated that the membrane enzyme, phospholipase A2, upregulates lysophospholipds that promote pore formation between synaptic vesicles and synaptic terminals. Therefore, the cell will employ the use of membrane proteins to increase the amount of certain lipids, which then influence secretory processes such as neurotransmission. These findings provide support that the interaction between membrane proteins and lipids is beyond structural. Therefore, it is pertinent to our understanding of the secretory process to investigate the interactions between non structural membrane lipids, specifically cholesterol and LPC, on SNARE complex disassembly.

Experimental Overview

The association between LPC- or cholesterol-associated t-SNARE and v-SNARE liposomes in the presence of NSF-ATP was examined using atomic force microscopy (AFM), dynamic light scattering (DLS), and X-ray diffraction measurements. Further, the disassembly of t-/v-SNAREs in isolated nerve terminals (fast secretor, ms) and exocrine pancreas (slow secretor, min) exposed to either cholesterol or LPC, was immunochemically determined. Since vesicle size influences membrane curvature, a

www.manaraa.com

uniform vesicle population was prepared for the entire study, using a published2 extrusion method. Two sets of 50 nm in diameter liposomes, one set containing cholesterol and the other LPC, were reconstituted with either t-SNARE or v-SNARE for use.

Detailed Materials and Methods

Preparation of t-SNAREs, v-SNARE and NSF: N-terminal 6xHis-tag constructs for SNAP-25 and NSF, C-terminal 6xHis-tag constructs for Syntaxin 1A and VAMP2 were generated. All four proteins were expressed with 6xHis at full length in E. coli (BL21DE3) and isolated by Ni-NTA (nickel-nitrilotriacetic acid) affinity chromatography (Qiagen, Valencia, CA). Protein concentration was determined by BCA assay.

Preparation of Proteoliposomes: All lipids were obtained from Avanti Polar Lipids (Alabaster, AL). For the control group, a 5 mM lipid stock solution was prepared by mixing lipid solution in chloroform-DOPC (1,2-dioleoyl phosphatidylcholine): DOPS (1,2-dioleoyl phosphatidylserine) in 70:30 mol/mol ratios in glass test tubes. For the cholesterol group, a 5 mM lipid stock solution was prepared by mixing lipid solution in chloroform-DOPC (1,2-dioleoyl phosphatidylcholine): DOPS (1,2-dioleoyl phosphatidylserine): cholesterol in 63:27:10 mol/mol/mol ratios in glass test tubes. For the LPC group, 5 mM lipid stock solution was prepared by mixing lipid solution in chloroform-DOPC (1,2-dioleoyl phosphatidylcholine): DOPS (1,2-dioleoyl phosphatidylserine): LPC (L-α-Lysophosphatidlycholine) in 63:27:10 mol/mol/mol ratios in glass test tubes. The lipid mixture was dried under gentle stream of nitrogen and resuspended in 5mM sodium phosphate buffer, pH 7.5, by vortexing for 5 min at room temperature. Unilamellar vesicles were formed following sonication 50x at 10 sec per sonication, followed by extrusion, resulting in 50 nm vesicles. Typically, vesicles

www.manaraa.com

ranging in size from 45-50 nm in diameter were obtained as assessed by AFM and photon correlation spectroscopy. Two sets of proteoliposomes were prepared by gently mixing either t-SNARE complex (Syntaxin-1A-His6/SNAP-25-His6; final concentration 25 µM) or VAMP2-His6 (final concentration 25 µM) with liposomes (Cho et al., 2002d; Jeremic et al., 2004), followed by three freeze/thaw cycles to enhance protein reconstitution at the vesicle membrane.

Atomic force microscopy: Atomic force microscopy was performed on liposomes placed on mica surface. Liposomes were imaged using the Nanoscope IIIa AFM from Digital Instruments. (Santa Barbara, CA). Images were obtained in the "tapping" mode in fluid, using silicon nitride tips with a spring constant of 0.38 N.m-1, and an imaging force of <200 pN. Images were obtained at line frequencies of 2 Hz, with 512 lines per image, and constant image gains. Topographical dimensions of the lipid vesicles were analyzed using the software nanoscope IIIa4.43r8, supplied by Digital Instruments.

Wide-angle X-ray diffraction studies: Sixty microliters of 1 mM PC:PS-cholesterol or -LPC t- and v-SNARE reconstituted vesicle suspension was placed at the center of an X-ray polycarbonate film, mounted on an aluminum sample holder in a Rigaku RU2000 rotating anode X-ray diffractometer equipped with automatic data collection unit (DATASCAN) and processing software (JADE). Experiments were performed at 25°C. Samples were scanned with a rotating anode, using the nickel-filtered Cu Ka line (λ=1.5418 Å) operating at 40 kV and 150 mA. Diffraction patterns were recorded digitally with scan rate of 10º/min using a scintillation counter detector. The scattered X-ray intensities were evaluated as a function of scattering angle 2θ and converted into Å units, using the formula d (Å)= $\lambda/2\sin\theta$. To determine the influence of LPC and cholesterol on the interaction between t-SNARE and v-SNARE vesicles in presence of

www.manaraa.com

NSF, and the ability of ATP to disassemble the t-/v-SNARE complex, X-ray diffraction studies were performed (Figure 2). Recordings were made of vesicles in solution in the 1.54-5.9 Å diffraction range, and a broad diffraction pattern is demonstrated, spanning 2θ ranges 26.67-42.45° or d value of 2.1-3.3 Å. The diffractogram traces exhibit a pattern typical of short-range ordering in a liquid system, indicating a multitude of contacts between interacting vesicles, majority being in the 3Å region. X-ray studies demonstrate larger clusters and consequently much less diffraction by the LPC vesicles compared to cholesterol. Not surprising, the average distance between cholesterol-vesicles is shorter (3.05Å) compared to LPC (3.33Å).

Light Scattering Measurements: Kinetics of association and dissociation of t-SNARE and v-SNARE reconstituted vesicles in solution were monitored by right angle light scattering assay with excitation and emission wavelength set at 600 nm in a Hitachi F-2000 spectrophotometer (Jeremic et al., 2004). Equal volumes of t-SNARE (5 μM) and v-SNARE (5 μM) reconstituted vesicle suspension and NSF (1 μg/ml), were injected into the cuvette containing 700 μl of assay buffer (140 mM NaCl, 10 mM Hepes pH=7.4, 2 mM CaCl2) at a final lipid concentration of 100 μM at 37°C. ATP-Mg (150 μM) was added to the mixture under continuous stirring, and changes in the light scattering were continuously monitored for a 5 min period. Values are expressed as intensities of scattered light (arbitrary units) taken continuously after addition of ATP, after which interactions between vesicles in solution reached a steady state. Student's t-test was used for comparisons between groups with significance established at $p<0.05$ (*).

Total brain homogenate preparation: Total brain homogenate was prepared from rat brains according to published methods (Cho et al., 2004; Cho et al., 2007). Whole brain, from Sprague-Dawley rats weighing 100-150 g, was isolated and placed in ice-

www.manaraa.com

cold buffered sucrose solution (5 mM Hepes, pH 7.4, 0.32 M sucrose). The brain tissue was sliced into small sections (approximately 0.5mm3) for immunoblot analysis.

Pancreas tissue preparation: Pancreatic tissue was isolated from Sprague-Dawley rats weighing 100-150 g according to published methods (Schneider et al., 1997). Tissue sections approximately 0.5mm^3 were prepared for immunoblot analysis.

Immunoblot Analysis of SNARE complex disassembly: Quantitative assessment of SNARE complex disassembly was determined using immunochemical analysis. Isolated rat brains (total brain homogenate) were stimulated using 30 mM KCl following exposure to cholesterol, LPC, or vehicle (control), followed by solubilization in buffer containing 1% Triton-1% Lubrol, 5mM ATP-EDTA in PBS. Similarly, pancreatic lobules exposed to 10 µM cholesterol, 10 µM LPC, or vehicle (control), was stimulated using 1µM carbamylcholine for different periods, followed by solubilization in buffer containing 1% Triton-1% Lubrol, 5mM ATP-EDTA in PBS supplemented with protease inhibitor cocktail (Sigma-Aldrich, St. Louis, MO). Interactions were stopped by addition of Laemmli reducing sample preparation buffer at R.T. and the SNARE complexes formed were resolved in a 12.5% SDS-PAGE. Proteins were electrotransferred to nitrocellulose sheets for immunoblot analysis using SNAP-25 (total brain homogenate) or SNAP-23 (exocrine pancreas) specific antibody (1:2000) (Alomone lab, Israel). Immunobands were visualized using a chemiluminescence detection system (Amersham Biosciences, UK) and photographed using a Kodak Image Station 440. Densytometric analysis of the immunobands was performed using the Kodak 1D Image Analysis software and is presented as relative intensities or optical density (O.D.). The approximately 70 to 75 kDa band is the t-/v-SNARE complex, and the lower 25 kDa and 23 kDa bands that of SNAP-25 and SNAP-23 respectively.

www.manaraa.com

Results and Discussion

t-/v-SNARE complexes formed between t- and v-SNARE reconstituted 50 nM liposomes displayed marked differences between cholesterol and LPC groups. SNARE complexes formed between cholesterol containing liposomes (Figure 13A, B) disassembled in the presence of NSF-ATP (Figure 13C). Conversely, SNARE complexes formed between LPC containing t- and v-SNARE reconstituted liposomes (Figure 13D, E, F) remained clustered in the presence of NSF-ATP (Figure 13G, H). These observations support the notion that LPC allows an initial secretory event while preventing subsequent secretions by SNARE complex disassembly inhibition.

To further determine the influence of LPC and cholesterol on the interaction between t-SNARE and v-SNARE vesicles in presence of NSF, and the ability of ATP to disassemble the t-/v-SNARE complex, X-ray diffraction studies were performed (Figure 14). Recordings were made of vesicles in solution in the 1.54-5.9 Å diffraction range, and a broad diffraction pattern was demonstrated, spanning 2θ ranges 26.67-42.45° or d values of 2.1-3.3 Å. The diffractogram trace exhibits a pattern typical of short-range ordering in a liquid system, indicating a multitude of contacts between interacting vesicles, the majority being in the 3Å region. In agreement with our AFM studies, X-ray studies demonstrate larger clusters and consequently much less diffraction by the LPC vesicles compared to Chol. However, the distance between vesicles is closer in the Chol population (3.05Å) compared to the LPC (3.33Å).

Dynamic light scattering (DLS) experiments were conducted to further support the findings from AFM and X-ray diffraction studies. Unassociated vesicles diffract more light in DLS experiments versus their aggregate counterparts. LPC-associated-t-/v-SNARE liposome complexes demonstrated a complete inhibition of NSF-ATP

www.manaraa.com

induced complex disassembly as compared to cholesterol-associated t-/v-SNARE lipsosome complexes (Figure 15A). The percent change in light scattering intensity was much greater in cholesterol groups versus LPC groups (Figure 15A), confirming the inability of LPC-associated complexes to disassemble in the presence of NSF-ATP. Upon analysis of real time light scattering measurements of LPC versus cholesterol-associated SNARE complexes, the kinetics show that LPC-associated-t-/v-SNARE liposome complexes dissociate at a much slower rate (k = 0.01) (Figure 15C) as compared to their cholesterol-associated counterparts (k = 0.03) (Figure 15B).

Additionally, stimulated brain slices and pancreatic tissue preparations displayed differences in SNARE complex disassembly between control, cholesterol and LPC groups (Figure 15D). Immunoblot analysis of stimulated tissue samples (both brain and pancreatic tissue) exhibit an inhibition of NSF-ATP induced SNARE complex disassembly in LPC incubated tissue samples versus control and cholesterol groups (Figure 15D). Membrane probed for SNAP protein (SNAP-25 in brain and SNAP-23 in pancreas) clearly demonstrate that the addition of LPC to tissue preparations causes an enrichment of the SNARE complex band in comparison to the other groups. Simultaneously, as the SNARE complex band increases, there is a corresponding decrease in the SNAP band, indicating that NSF-ATP stimulated dissociation is not occurring (Figure 15D). Therefore, LPC has an inhibitory effect on NSF-ATP induced SNARE complex disassembly and these results are consistent with both AFM and X-ray diffraction analyses (Figure 13 and Figure 14).

Collectively, these studies provide support for the postulation that LPC is a secretion inhibitor. In the presence of LPC, SNARE complexes are still able to associate (Figure 13E, F); however, disassembly of the complex via NSF-ATP is

www.manaraa.com

abrogated (Figure 13G, H). This finding suggests that an initial secretion event can occur in the presence of LPC but that additionally rounds of secretion cannot. Furthermore, it appears that cholesterol does not have the same effect on SNARE complex disassembly. Liposomes in the presence of cholesterol seem to behave similarly to control groups (Figure 15D) in that SNARE complex disassembly is not interfered with as it is in LPC groups. This result is in agreement with previous studies that show that cholesterol depletion from isolated synaptic membranes does not affect SNARE complex assembly (Cho et al., 2007).

These studies reinforce a deeper connection between membrane proteins and lipids. Not only can membrane lipids influence protein interactions, proteins can stimulate an increase in specific lipids such as lysophopholipids, which can influence processs such as secretion (Zimmerberg and Chernomordik, 2005). As was previously discussed, LPC is upregulated in cancer (Sutphen et al., 2004; Fang et al., 2000) and drawing on this association, a greater understanding of lipid protein interactions can be useful targets for treatment.

www.manaraa.com

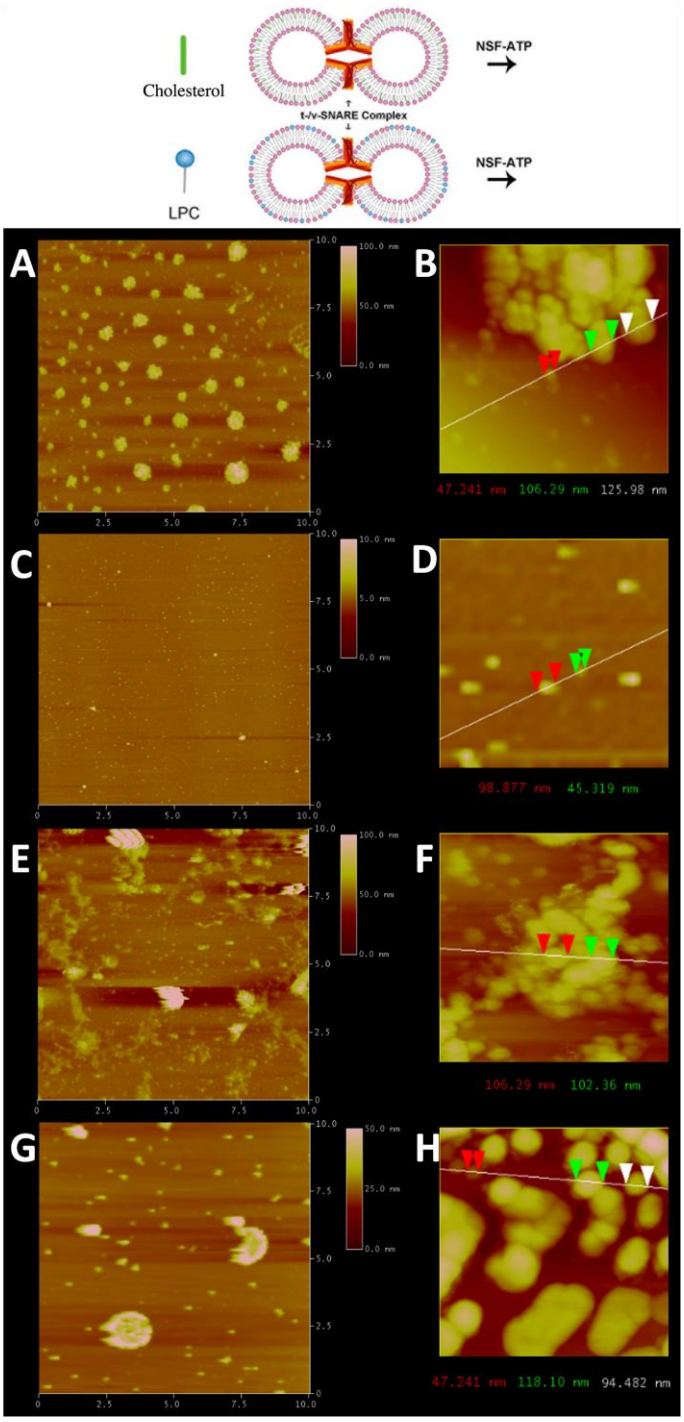

Figure 13. Representative AFM micrographs demonstrating LPC containing t-/v-SNARE proteoliposome complexes fail to dissociate in presence of NSF-ATP. Top panel is a schematic outline of the experiment. Exposure of cholesterol-associated t-SNARE and v-SNARE liposome mixtures (A, B, low and high magnification) to NSF-ATP results in liposome dissociation as demonstrated in C (at low magnification) and D (at higher magnification). In contrast, LPC-associated t-/v-SNARE liposomes (E, F) remain clustered (G, H) following exposure to NSF-ATP.

www.manaraa.com

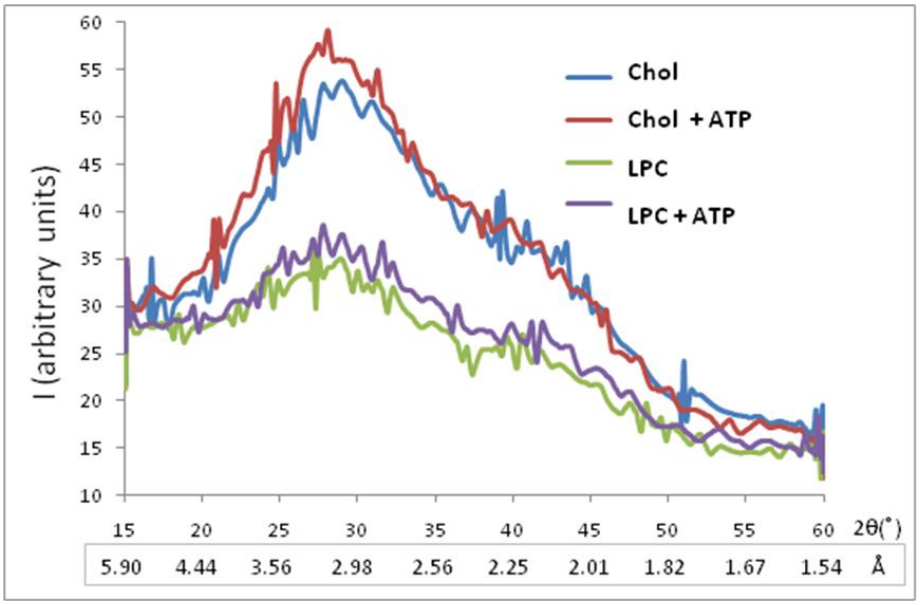

Figure 14. Wide-angle X-ray diffraction pattern of interacting lipid vesicles. Diffraction profiles of a mixture of 50 nm in diameter t-SNARE and v-SNARE reconstituted PC:PS vesicles either containing cholesterol (Chol.) or lysophosphatidylcholine (LPC), in presence of NSF. Exposure of the Chol vesicles to ATP results in t-/v-SNARE disassembly by the NSF and an increase in the vesicle-vesicle contact distance from 3.05Å (-ATP) to 3.13Å (+ATP), as opposed to LPC from 3.33Å (-ATP) to 3.23Å (+ATP). Note as a consequence of clustering, while diffraction is significantly lower in the LPC vesicles (lower green peak), the distance between vesicles is closer between the Chol population.

www.manaraa.com

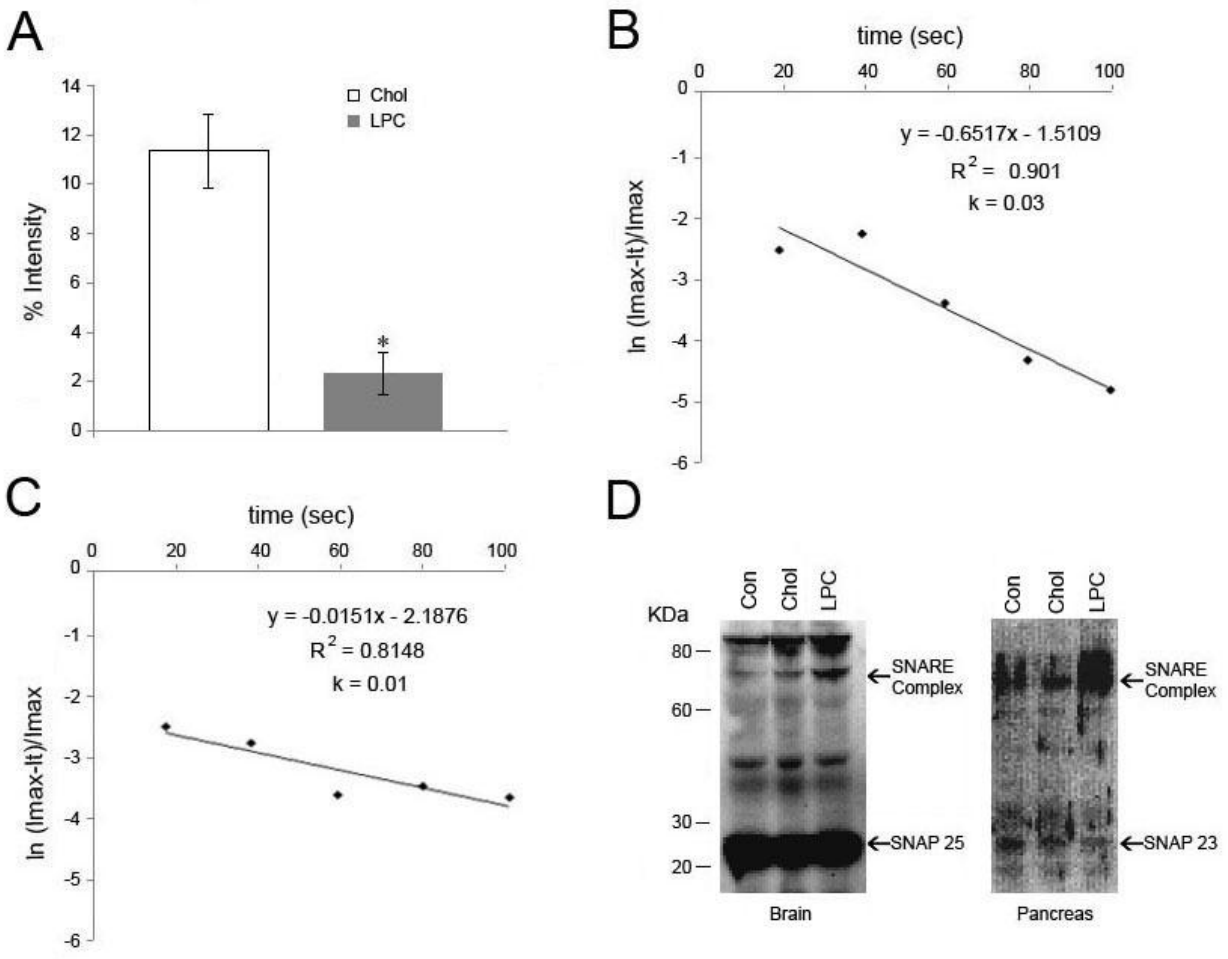

Figure 15. SNARE complexes in presence of LPC fail to disassemble. (A) Real-time dynamic light scattering (DLS) profiles on cholesterol-associated (CHOL) and LPC-associated t-/v-SNARE liposomes in presence of NSF-ATP. There is no appreciable dissociation of the LPC vesicles, in contrast to a rapid ATP-dependent dissociation of CHOL vesicles. (B) Note the dissociation of cholesterol-associated t-/v-SNARE vesicles occurs with rate constant k = 0.03 s-1, and (C) a relatively slow dissociation in LPC vesicles. (D) Following KCl stimulation, when isolated synaptosomes are solubilized in buffer containing ATP-EDTA, resolved by SDS-PAGE, followed by immunoblot analysis using SNAP-25 specific antibody, negligible disassembly of the t-/v-SNARE complex is demonstrated in the LPC group as opposed to the control and the CHOL group. Similarly in the presence of LPC, there is little disassembly of the t-/v-SNARE complex in the exocrine pancreas following stimulated secretion using 1μM carbamylcholine.

www.manaraa.com

CHAPTER 4

INVOLVEMENT OF vH^+-ATPASE IN SYNAPTIC VESICLE SWELLING

INTRODUCTION

Although vesicle docking to porosomes rationalizes the appearance of partially empty vesicles following a secretory stimulus (Cho et al., 2002a), simple diffusion of intravesicular contents once membrane continuity is established, cannot account for the sub-microsecond time scale characteristic of neuronal transmission. Given this dilemma, the cell must employ a mechanism by which vesicular contents are rapidly discharged in a regulated manner. The first direct measurement of secretory vesicle swelling at nanometer resolution within live cells was reported in studies on pancreatic acinar cells, using atomic force microscopy (Cho et al., 2002c). Recent studies have indicated the secretory requirement for vesicle swelling through a GTP stimulated $G_{\alpha o}$ signaling cascade, which culminates in water entry through activated aquaporin channels in the vesicle membrane (Kelly et al., 2004; Jeremic et al., 2005). This regulated signaling cascade provides an explanation for the cell's employment of a coordinated mechanism for intravesicular expulsion versus passive diffusion of contents out of the cell.

Multiple studies have indicated that mastoparan, an amphiphilic tetradecapeptide from wasp venom, stimulates the GTPase activity of $G_{\alpha o/i}$ proteins (Higashijima et al.1988; Vitale et al., 1993; Konrad et al., 1995). The activation of G proteins is proposed to occur through the insertion of mastoparan into the lipid bilayer, resembling the intracellular loops of G-protein-coupled receptors. The ability of mastoparan to initiate the $G_{\alpha o}$ signaling cascade involved in synaptic vesicle swelling confirms its essential use for GTP induced swelling stimuli.

www.manaraa.com

Previous findings demonstrate that vH^+-ATPases are present in synaptic vesicle membranes (Stadler & Tsukita, 1984; Hicks & Parsons, 1992) and are responsible for the formation of an intravesicular electrochemical H^+ gradient (pH 5.2-5.5) (Michaelson & Angel, 1980; Füldner & Stadler, 1982), required for transport of neurotransmitters into the vesicle lumen. Additionally, vH^+-ATPases have also been shown to participate in neurotransmitter secretion (Morel et al., 2001; Peters et al., 2001). Furthermore, guanine nucleosides have been reported to influence the glutamate-induced cellular response via diverse trophic, proliferative, and modulatory effects of the nucleotide on neurons (Santos et al., 2005). Because synaptic vesicle swelling is Gao mediated and is required for cell secretion (Kelly et al., 2004), the vH^+-ATPase in synaptic vesicle membranes (Stadler and Tsukita, 1984; Hicks and Parsons, 1992) may participate in Gao-mediated water gating through the AQP-6 channels at the synaptic vesicle membrane, resulting in vesicle swelling. Due to the extensive evolvement of vH^+-ATPases in secretory processes, investigation into the molecular dynamics of these channels is essential to our understanding of the mechanisms of cell secretion.

Experimental Overview

Synaptic vesicles were isolated from whole rat brain preparations. Synaptic vesicle size changes were monitored both by photon correlation spectroscopy (PCS) and dynamic light scattering techniques. Vesicle samples were administered GTP-mastoparan to induce swelling both with and without the vH^+-ATPase inhibitory molecule, bafilomycin (BM). In addition to the inhibition of vH^+-ATPase activity, vesicles were induced to swell (using GTP-mastoparan) under different pH conditions. Potential measurements were also collected to determine the change in surface charge under different pH conditions with and without GTP-mastoparan stimulation.

www.manaraa.com

Detailed Materials and Methods

Synaptosome and synaptic vesicle isolation. Synaptosomes and synaptic vesicles were prepared from rat brains using published procedures (Kelly et al., 2004; Jeremic et al., 2005). Whole brain from Sprague-Dawley rats, weighing 100-150 g, was isolated and placed in ice-cold buffered sucrose solution (5 mM Hepes pH 7.5, 0.32 M sucrose), supplemented with protease inhibitor cocktail (Sigma, St. Louis, MO). The brain tissue was homogenized using 8-10 strokes in a Teflon-glass homogenizer. The total homogenate was centrifuged for 3 min at 2,500 x *g*, and the supernatant fraction was further centrifuged for 15 min at 14,500 x *g*, to obtain a pellet. The resultant pellet was resuspended in buffered sucrose solution, and loaded onto a 3-10-23 % Percoll gradient. After centrifugation at 28,000 x *g* for 6 min, the enriched synaptosome fraction was collected at the 10-23 % Percoll gradient interface. To isolate synaptic vesicles, the synaptosome preparation was diluted using 9 vol. of ice-cold water, resulting in the lysis of synaptosomes to release synaptic vesicles, followed by 30 min incubation on ice. The homogenate was then centrifuged for 20 min at 25,500 x *g*, and the resultant supernatant enriched in synaptic vesicles was obtained.

Transmission electron microscopy. Isolated synaptic vesicle preparations were fixed in 2.5% buffered paraformaldehyde for 30 min, followed by dehydration and embedding in Unicryl resin. The resin-embedded tissue was sectioned at 40-70 nm. Thin sections were transferred to coated specimen TEM grids, dried in the presence of uranylacetate and methylcellulose, and examined in a JOEL transmission electron microscope.

Synaptic vesicle size measurements using photon correlation spectroscopy. Changes in synaptic vesicle size were determined using photon correlation spectroscopy (PCS). PCS is a well-known technique for the measurement of size of

www.manaraa.com

micron to nm size particles and macromolecules. PCS measurements were performed in a Zetasizer Nano ZS, (Malvern Instruments, UK). In a typical experiment, the size distribution of isolated synaptic vesicles was determined using built-in software provided by Malvern Instruments. Prior to determination of the vesicle hydrodynamic radius, calibration of the instrument was performed using latex spheres of known size. In PCS, subtle fluctuations in the sample scattering intensity are correlated across microsecond time scales. The correlation function was calculated, from which the diffusion coefficient was determined. Using Stokes-Einstein equation, hydrodynamics radius can be acquired from the diffusion coefficient (Higashijima et al., 1988). The intensity size distribution, which is obtained as a plot of the relative intensity of light scattered by particles in various size classes, is then calculated from a correlation function using built-in software. The particle scattering intensity is proportional to the molecular weight squared. Volume distribution can be derived from the intensity distribution using Mie theory (Vitale et al., 1993; Weingarten et al., 1990). The transforms of the PCS intensity distribution to volume distributions can be obtained using the provided software by Malvern Instruments. In experiments, isolated synaptic vesicles were suspended in isotonic buffer containing 0.3 M Sucrose, 10 mM Hepes pH 7.5, and 20 mM KCl, and changes in vesicle size monitored prior to and after addition of 40 mM GTP-mastoparan, and or 1 nM bafilomycin. Student's *t*-test was performed for comparison between groups (n=5) with significance established at $p<0.05$(*).

Measurements of synaptic vesicle size using right angle light scattering. Similar to PCS, isolated synaptic vesicles were suspended in isotonic buffer (0.3 M Sucrose; 10 mM Hepes pH 7.5; and 20 mM KCl) and changes in vesicle size monitored prior to and following the addition of 40 mM GTP-mastoparan, and or 1 nM bafilomycin. Synaptic

www.manaraa.com

vesicle size dynamics were determined using real time right angle light scattering, in a Hitachi F-2000 spectrofluorimeter. Scattered light intensities at 600 nm were measured as a function of vesicle radius (Cho et al., 2004). Values are expressed in arbitrary units and as percent light scattered over controls. Student's *t*-test was performed for comparison between groups (n=5) with significance established at $p<0.05$(*).

Synaptic vesicle acidification determined from zeta potential measurements. Zeta potential is the overall surface charge a particle acquires in a certain medium. Hence in the case of liposomes or isolated synaptic vesicles in aqueous media, the zeta potential is a direct reflection of both the internal and external pH of vesicles. If more alkali buffer is added to the vesicle suspension, then the vesicles acquire more negative charge. In contrast, if acid is added to the suspension, the vesicles acquire less negative charge. This implies that the pH of the buffer both within and outside the vesicle, dictates the zeta potential or the net surface charge of the vesicle. Experiments were performed on isolated synaptic vesicles suspended in isotonic buffer containing 0.3 M sucrose, 10 mM Hepes pH 7.5, and 20 mM KCl, and changes in vesicle zeta potential monitored prior to and after addition of 40 mM GTP-mastoparan, and or 1 nM bafilomycin. Zeta potential was determined using the Zetasizer Nano ZS, from Malvern Instruments, UK. Student's *t*-test was performed for comparison between groups (n=8) with significance established at $p<0.001$(*).

Atomic force microscopy. Isolated synaptosome membrane or synaptic vesicles in buffer were plated on freshly cleaved mica, to be imaged using the atomic force microscope (AFM). Ten minutes after plating, the mica disk was placed in a fluid chamber and washed with the incubation buffer to remove unattached membrane and or synaptic vesicles, prior to imaging in the presence or absence of 40 mM GTP-

www.manaraa.com

mastoparan, and or 1 nM bafilomycin. Isolated synaptosome membrane and synaptic vesicles were imaged using the Nanoscope IIIa, Digital Instruments (Santa Barbara, CA). All images presented in this study were obtained in the ‘‘tapping’’ mode in fluid, using silicon nitride tips with a spring constant of 0.06 Nm^{-1} and an imaging force of less than 200 pN. Images were obtained at line frequencies of 2.523 Hz, with 512 lines per image and constant image gains. Topographical dimensions of synaptic vesicles were analyzed using the NANOSCOPE (R) IIIA 4.43r8 software, supplied by Digital Instruments.

Immunoblot analysis. Protein content in the various brain fractions, were determined by the Bradford method (Bradford, 1976). Sample aliquots solubilized in Laemmli (Laemmli, 1970) sample preparation buffer, were resolved using 12.5% SDS-PAGE. Five micrograms protein, each from total brain homogenate, synaptosome, and synaptic vesicle fractions, were resolved using SDS-PAGE. Resolved proteins were electrotransferred to nitrocellulose membrane for immunoblot analysis using specific antibodies to VAMP-2 (Alomone Labs, Jerusalem, Israel), vH^+-ATPase and AQP-6 from the Aquaporins1-9 kit (a□Diagnostic, San Antonio, TX). The nitrocellulose membranes electrotransferred with the resolved proteins were incubated for 1 h at 4ºC in blocking buffer (5% non-fat milk in PBS containing 0.1% Triton X-100 and 0.02% NaN_3), and immunoblotted for 1 h at room temperature with the specific antibody. Primary antibodies were used at a dilution of 1:3,000 (VAMP-2); 1:1000 AQP-6 and vH^+-ATPase) in blocking buffer. The immunoblotted nitrocellulose sheets were washed in PBS containing 0.1% Triton X-100 and 0.02% NaN_3 and incubated for 1 h at room temperature in horseradish peroxidase-conjugated secondary antibody at a dilution of 1:3,000 in blocking buffer. The immunoblots were then washed in PBS buffer,

www.manaraa.com

processed for enhanced chemiluminescence (Amersham Biosciences, NJ) and developed using a Kodak 440 image station.

Results and Discussion

EM, AFM, immunoblot analysis, and PCS all confirmed the purity of the obtained synaptic vesicle preparation (Figure 16). Size profiles for the sample indicated an average size of 35 nm and immunoblot data demonstrated an enrichment of the synaptic vesicle specific proteins, VAMP-2 and AQP-6 in synaptic vesicle fractions (Figure 16C). As indicated from previous studies (Stadler and Tsukita, 1984; Hicks and Parsons, 1992), immunoblot data also confirmed the presence of vH^+-ATPases in both synaptosome and synaptic vesicle samples, with enrichment in the latter (Figure 16C). Collectively, these experiments demonstrate the isolation of a highly enriched SV preparation from brain tissue for SV swelling assays.

To determine the relative concentration of vH1- ATPase in SV, immunoblot analysis was performed with 5 µg each of total brain homogenate (BH), isolated synaptosome (S), and SV fractions (Fig. 20C). In agreement with earlier findings (Stadler and Tsukita, 1984; Hicks and Parsons, 1992), vH1-ATPase was present both in the S and in the SV fraction but was enriched in SV (Fig. 20C). Dynamic light scattering profiles indicated 0.5 nm BM as the optimal concentration for inhibition (approximately 25%) of GTP-mastoparan stimulated SV swelling (Figure 17A). Additionally, light scattering and PCS experiments revealed that SV exposure to BM alone caused a decrease in SV size (~18-20%) (Figure 17B) and BM + GTP-mastoparan had an abated swelling response as compared to GTP-mastoparan alone (Figure 17A, B). In corroboration with these findings, AFM analyses indicated similar results confirming an inhibition of GTP-mastoparan stimulated synaptic vesicle swelling in the presence of BM

www.manaraa.com

(Figure 18). Because of the decrease in GTP-mastoparan induced swelling, these data indicate vH^+-ATPases to be upstream of the AQP-6 channel. Also, water entry into vesicles is only partially regulated by vH^+-ATPases as indicated by the slight but not complete inhibition of the swelling response (Figure 17A, B). It is highly possible that water entry into vesicles is a consequence of the electrochemical H^+ gradient produced by vH^+-ATPases for intravesicular neurotransmitter uptake.

Former investigations into cellular acidification and its effects on vH^+-ATPases reveal profound effects on localization and activity of these transporters (Alexander et al., 1999; Nordstrom et al., 1997). Exposure to moderately acidic extracellular pH (pH 6.5) augments plasmalemmal vH^+-ATPase activity in cultured osteoclasts (Nordstrom et al., 1997). In addition, some studies (Bastani et al., 1991, 1994; Chambrey et al., 1994) report that the number of vH^+-ATPase in apical membrane of renal epithelial cells is up-regulated in animals exposed to acidosis (Bastani et al., 1991, 1994; Chambrey et al., 1994). Therefore, elucidating the effects of pH environment on synaptic vesicle swelling was also examined in the current study. PCS and light scattering results demonstrated complete inhibition of $G_{\alpha o}$-mediated SV swelling under even slightly acidic or alkaline conditions (Figure 17C, D). The GTP-mastoparan-stimulable SV swelling was found to be rapid (Fig. 21E), as opposed to SV swelling in hypotonic medium. No change in SV size was found up to 105 sec following exposure to a 50% hypotonic buffer (data not shown). Insofar as bafilomycin is specific in its inhibition of vH^+-ATPase, this pH sensitivity of SV swelling may be a reflection of the direct inhibition of vH^+-ATPase activity under both basic and acidic conditions (Fig. 21B–D). This data provides confirmation that SV swelling is pH sensitive.

The activity of vH^+-ATPases in the efficacy of SV swelling was also analyzed

www.manaraa.com

utilizing kinetic data collected from dynamic light scattering experiments (Figure 17E). GTP-mastoparan induced swelling was determined to be first order with a rate constant k = 0.0106 sec^{-1} as compared to k = 0.0068 sec^{-1} in the presence of bafilomycin (an approximate 35% inhibition). Results from the study demonstrate that bafilomycin exposure decreases both the potency and the efficacy of GTP-Mas-induced SV swelling by 20% and 35%, respectively. These findings indicate a strong correlation between AQP-6 and vH^+-ATPase activity in synaptic vesicle swelling.

Further confirmation of the inhibition of GTP-mastoparan stimulated increase in isolated SV volume following exposure to bafilomycin was demonstrated by using AFM (Figure 18). Exposure of SV to 40 lM GTP-mastoparan demonstrated a robust increase in vesicle size (Figure 18A). However, prior exposure of SVs to 1 nM bafilomycin resulted in a significant (*P < 0.001) inhibition of the GTP-mastoparan-induced swelling of synaptic vesicles (Figure 18B, C).

To determine bafilomycin's effect on synaptic vesicle acidification, zeta potential measurements were collected on SVs in varying pH environments under stimulation of GTP-mastoparn (Figure 19). Isolated SVs were negatively charged at approximately -20 to -25 mV. As vesicles lost acidity, net membrane charge became more positive. Under stimulation by GTP-mastoparan, vesicle membrane decreased in negativity (–24.4 ± 2.1 to –12.3 ± 1.0). In the presence of bafilomycin, GTP-mastoparan stimulated decrease in acidity was diminished (Figure 19A). In either highly alkaline or acidic buffer, SVs failed to respond to GTP-mastoparan stimulation (Figure 19B). Both acidic and basic suspension media inhibited vH^+-ATPase activity, thereby preventing the entry of protons into the vesicle lumen. Results from these studies support the idea that luminal acidification of SV is a requirement for AQP-6-induced active water transport

www.manaraa.com

and vesicle swelling and that either low (pH 4) or high (pH 8) pH inhibits the activity of SV-associated vH^+-ATPase (Figure 19). However, G_{ao}-stimulated SV acidification is completely abrogated (Figure 19A) and bafilomycin is able to inhibit only partially the G_{ao}-stimulated SV swelling (Figure 17B), suggesting that vH^+-ATPase is in part responsible for the G_{ao}-mediated SV swelling.

Collectively, these studies demonstrate the integral role of vH^+-ATPases in G_{ao}-mediated SV swelling. Water channels including AQP-6 are bidirectional, and the vH^+-ATPase inhibitor bafilomycin decreases the volume of resting synaptic vesicles, suggesting vH^+-ATPase to be upstream of AQP-6, in the pathway leading from Gao-stimulated swelling of synaptic vesicles (Figure 20). Not only is the proton transporter itself necessary in the activation of the swelling pathway, it is also inhibited by changes in pH environment of the cell; indicating that pH can also influence the swelling response and modulate cell secretion. Vesicle acidification is therefore a prerequisite for AQP-6-mediated rapid gating of water into synaptic vesicles.

www.manaraa.com

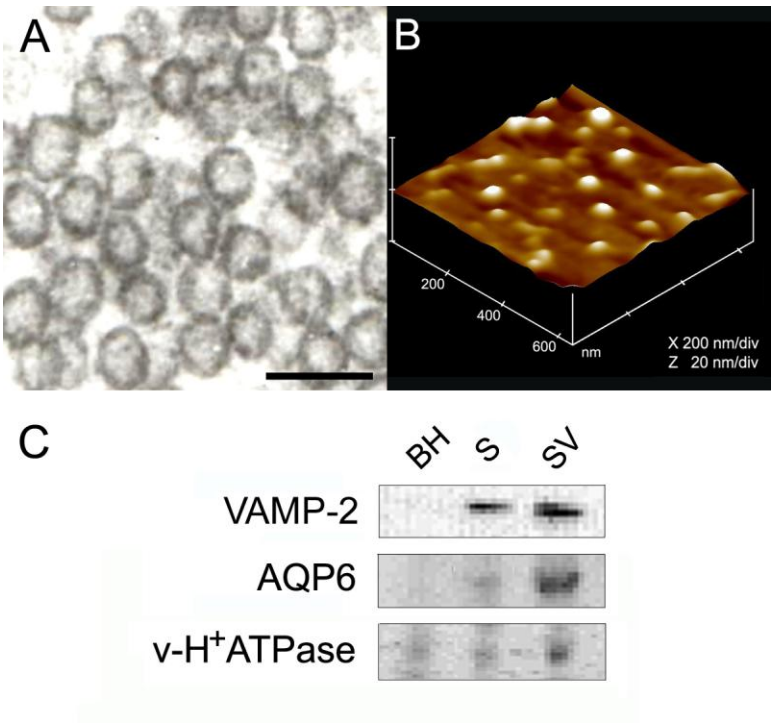

Figure 16. Associate of vH^+-ATPase with synaptic vesicles. Purity of synaptic vesicles was determined by using transmission electron microscopy (A), atomic force micrscopy (B), and immunoblot analysis (C) on isolated synaptic vesicles. Both electron and atomic force micrographs demonstrate the average size of synaptic vesicles to be 40 nm, which is futher confirmed by photon correlation spectroscopy in Figure 17. Immunoblot analysis of 5 µg protein each of total rate brain homogenate (BH), synaptosome (S), and synaptic vesicles (SV) demonstrates the enriched presence of SV proteins VAMP-2 and the water channel AQP6. Note the enriched presence of vH^+-ATPase in the SV fraction. Scale bar = 100 nm. (Shin et al., 2009)

www.manaraa.com

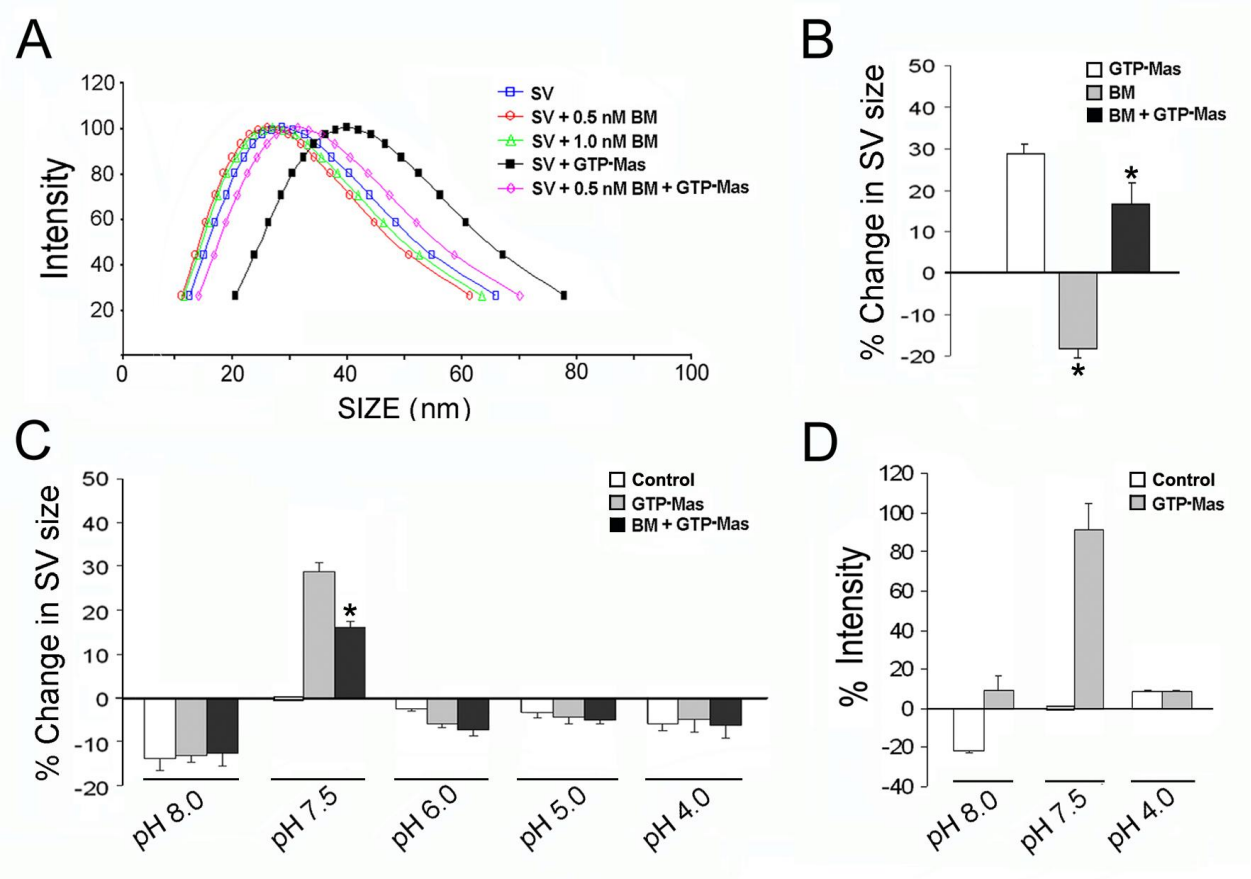

Figure 17. A-E: Guanosine triphosphate-mastoparan (GTP-MAS) induced synaptic vesicle (SV) swelling is both pH and bafilomycin (BM) sensitive. Isolated SV's swell in response to 40 µM GTP-Mas, as demonstrated by using photon correlation spectroscopy (A-C). Similarity, right-angle light scattering also demonstrates an increase in SV size following exposure to the GTP-Mas mixture. Exposure of SV to 0.5 or 1 nM of the vH^+-ATPase inhibitor BM or low pH significantly inhibits GTP-Mas induced vesicle swelling (A-D). Note the loss in SV size following exposure to BM alone (B). The GTP-Mas induced SV swelling is pH sensitve (C), insofar as, except the near physiological pH of 7.5, both alkaline and acidic environments nearly abolish GTP-Mas-induced swelling of SV, as determined both by photon correlation spectroscopy (C) and by dynamic light scattering measurements (D). B-D: n = 5, *P<0.001. (Shin et al., 2009)

www.manaraa.com

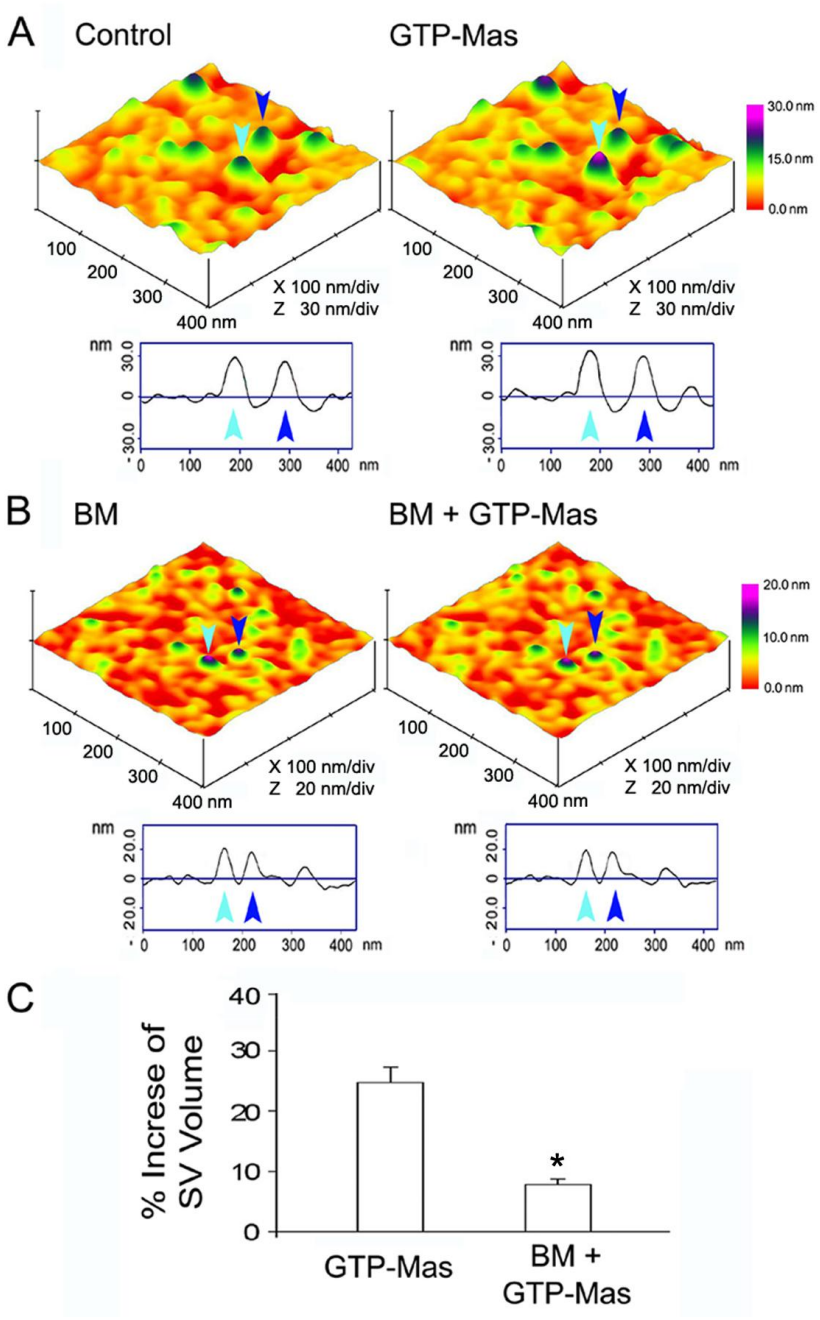

Figure 18. Atomic force microscopy on synaptic vesicles demonstrating inhibition of GTP-Mas-induced synaptic vesicle (SV) swelling by bafilomycin (BM). In accordance with photon correlation spectroscopy and dynamic light scattering studies (Fig. 2), isolated SVs (A, left) swell when exposed to 40 µM GTP-Mas (A, right). Exposure of SV to 1 nM of the vH^+-ATPase inhibitor BM (B, left) significantly inhibits GTP-Mas-induced vesicle swelling (B, right). Note the loss in GTP-Mas-induced SV volume increase following exposure to BM (C); n = 22, *P < 0.001. (Shin et al., 2009)

www.manaraa.com

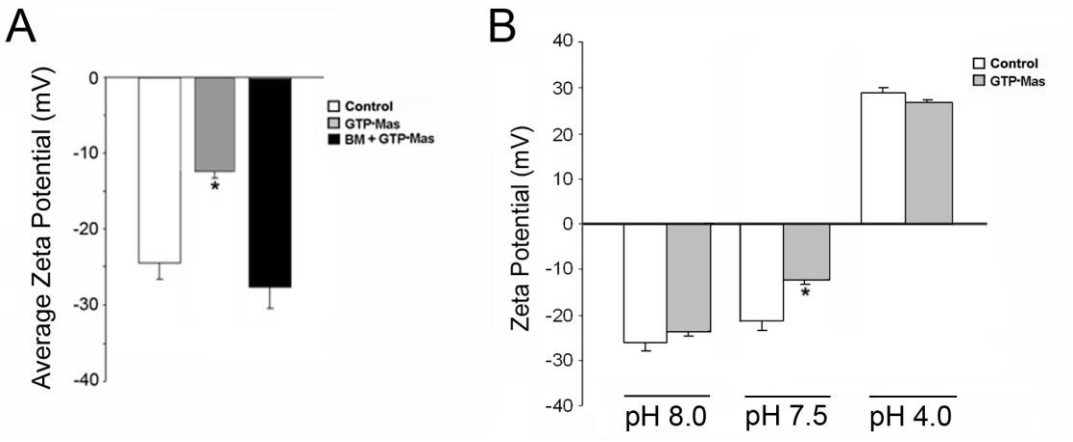

Figure 19. Exposure of SVs to the vH^+-ATPase inhibitor bafilomycin abrogates the GTP-Mas-induced net loss in negative charges at the vesicle membrane by inhibiting vesicle acidification. A: With the exception of pH 7.5, vesicles in either acidic or alkaline medium fail to elicit any change in their zeta potential (B), demonstrating that both acidic and basic suspension media inhibited vH^+-ATPase activity, thereby preventing the entry of protons into the vesicle lumen. *P < 0.05. (Shin et al., 2009)

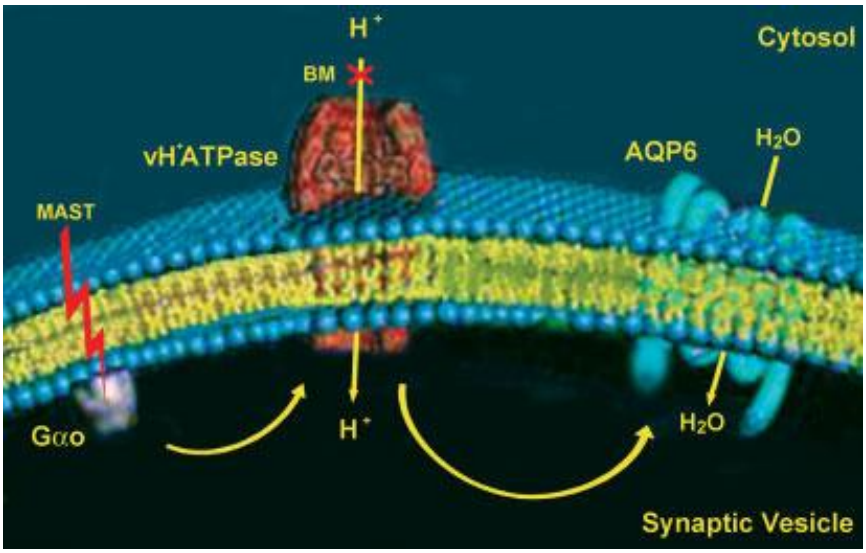

Figure 20. Diagram of the synaptic vesicle membrane depicting the presence of Gao, vH^+-ATPase, and the water channel AQP6. Mastoparan (MAST) stimulates GTP-Gao protein. This study demonstrates involvement of vH^+-ATPase in GTP-Gao-mediated synaptic vesicle swelling. Results demonstrate a bafilomycin (BM)-sensitive (red X) vesicle acidification following the GTP-Gao stimulus, and water channels are bidirectional and the vH^+-ATPase inhibitor BM decreases both the volume of isolated synaptic vesicles and GTP- mastoparan stimulated swelling, suggesting vH^+-ATPase to be upstream of AQP- 6. Vesicle acidification is therefore a prerequisite for AQP-6-mediated gating of water into synaptic vesicles. (Shin et al., 2009)

www.manaraa.com

CHAPTER 5

GENERAL DISCUSSION AND CONCLUSIONS

Due to the fact that hormone and neurotransmitter secretion out of cells is such a rapid and highly regulated process, and because total fusion of vesicular and cell lipid bilayers does not address these issues, cell secretion is an obvious resolution to these predicaments but had remained an enigma until recently. Previous studies have implicated the role of non-structural membrane lipids such as cholesterol and LPC in the secretory process; however, the precise mechanisms underlying these interactions were unknown. In a 2007 study by Cho and others, depletion of cholesterol from synaptosomal membranes resulted in a decrease in porosome integrity but had no effect on t-/v-SNARE complex assembly. It was however demonstrated in this study that interactions between t-SNAREs and associated calcium channels were disrupted. Because the presence of calcium is required for membrane fusion between secretory vesicle and cell plasma membrane, it follows that a disturbance in the interaction between SNAP-25, syntaxin-1 and calcium channels leads to an inhibition of secretion. Therefore, there is a lipid-protein interaction occurring between cholesterol and secretory complex proteins that is vital to the process of cell secretion.

Although the previous study had shown a requirement for cholesterol, specifically in interactions between SNARE proteins and other porosome proteins such as the calcium channel, it also demonstrated that cholesterol had no effect on the size, shape and assembly of the t-/v-SNARE complex. Furthermore, prior studies have shown a direct decrease in neurotransmission due to the depletion of cholesterol from synaptic membranes (Zamir and Charlton, 2006). Not only does cholesterol associate with porosome proteins, it also has interactions with proteins at the synaptic vesicle such as

www.manaraa.com

synaptophysin and VAMP. Although the function of synaptophysin is relatively unknown, it is understood that it has associations with the essential synaptic vesicle protein VAMP, and that this interaction may be mediated by cholesterol (Mitter et al., 2003).

Besides cholesterol, another non-structural membrane lipid, LPC, has also been shown to influence secretory processes. Isolated, perfused rat atria when administered LPC via the perfusate demonstrated a dose dependent decrease in ANP secretion (Han et al., 2003). Additionally, evidence has shown that low density lipoproteins (LDLs) accumulate at atherosclerotic regions of vasculature. These oxidized LDLs can then result in the insertion of LPC into endothelial cell membranes which can suppress the secretion of endothelin-1 from cultured vascular endothelial cells (Jougaski et al., 1992).

A main contributor to cardiovascular disease is arthrosclerosis due to poor diets that cause high plasma lipid concentrations (Watts et al., 1992). In a 1992 study by Watts and others, men with coronary artery disease were treated with either a low fat diet or the combination of low fat diet with the drug cholestyramine (responsible for lowering plasma cholesterol levels). From this study, it was determined that a reduction in dietary fat intake was sufficient to cause a regression in coronary artery disease. In patients treated with both diet and cholestyramine therapy, there was a net increase in coronary lumen diameter, which was a result of a decrease in atherosclerotic plaque. Because of the overall implications of high lipid diet and its effects on both cholesterol and LPC levels in the body, it is important to understand how these lipid molecules disrupt normal processes in the cell. Due to the accumulating evidence that both of these lipid molecules are involved in the secretory process, it is imperative to understand the molecular dynamics of the lipid-protein interaction which underlies these

www.manaraa.com

operations.

From the current study, we have been able to show that cholesterol has no effect on t-/v-SNARE complex assembly (Shin et al., 2010). These findings are consistent with previous study findings from Cho and others in 2007 and are a first time observation of the molecular folding events occurring in the SNARE complex in the presence of cholesterol. What was really surprising was the effect that LPC had on SNARE complex disassembly. In the presence of LPC, t-/v-SNARE complexes formed between t- and v-SNARE reconstituted liposomes did not disassemble in the presence of NSF-ATP. This was demonstrated by maintenance of α-helices within the complex (Table 1) (Shin et al., 2010). From these observations, it is clear that LPC has an inhibitory effect on SNARE complex disassembly; however, it allows for an initial binding event to occur between t- and v-SNAREs. This suggests that there is an initial complex formation and secretory event that occurs in the presence of LPC, yet further secretions are inhibited.

Although LPC is upregulated by the activity of phospholipase A2 (Zimmerberg and Chernomordik, 2005), the aforementioned study was done in liposomes without any exogenous proteins outside of t- and v-SNAREs. Therefore, it is reasonable to conclude that the effect shown is a result of LPC's direct action on the SNARE complex. The fact that LPC levels are however increased by phospholipase A2 activity brings to mind the idea that any process that is responsible for stimulating this inflammatory pathway may also cause disruption to secretory processes in the cell.

In conformation of the previous study, it was demonstrated that SNARE complex disassembly is inhibited, both in pancreatic (slow secretor) and brain (fast secretor) tissues, in the presence of LPC (Figure 13 and Figure 15). This was clearly

www.manaraa.com

demonstrated utilizing immunoblot analysis (Figure 15D). Additionally, the current study showed that when disassembly is stimulated (by NSF-ATP), the process occurs much more rapidly in cholesterol containing liposomes (Figure 15B).

Collectively, these studies indicate that LPC does indeed have an inhibitory effect on SNARE disassembly while cholesterol seems to maintain the secretory response in cells. To confirm the effects of cholesterol and LPC on the overall secretion process, these studies should be repeated in live cells and measurements of secretory products should be made to determine if the secretory response is abrogated in cells incubated with LPC. Initial studies using pancreatic tissue have begun and amylase secretion after treatment of tissue with cholesterol or LPC has been measured, but must be repeated for significance.

In addition to understanding the interaction of lipids with SNARE proteins, it would be pertinent to our understanding of the t-/v-SNARE protein complexes and their associations with membrane lipids to conduct a series of experiments utilizing truncated SNARE proteins. This would allow us the ability to determine which regions of the proteins are responsible for SNARE complex assembly and may also shed some insight into the interactions of the transmembrane regions of the SNARE proteins with the lipid bilayer.

As well as investigating the effects of cholesterol and LPC on SNARE complex assembly-disassembly, the current study looked at the swelling response of vesicles in different pH environments. It is well known that vH^+-ATPases are present in vesicle membranes (Stadler & Tsukita, 1984) and are required for vesicle acidification (Füldner & Stadler, 1982), which is itself necessary for uptake of intravesicular contents into the vesicle. Additionally, study findings have shown that vesicles swell or increase in size in

www.manaraa.com

response to stimulation by GTP and mastoparan, and that GTP stimulates a $G_{\alpha o}$ signaling cascade, that results in swelling due to water entry into the vesicle via aquaporin channels (Kelly et al., 2004; Jeremic et al., 2005). Upon inhibition of water channels, the swelling response is abrogated but not completely abolished (Cho et al., 2002c). This finding seems to suggest that the $G_{\alpha o}$ signaling cascade involves a number of proteins within the secretory vesicle membrane. Therefore, it was pertinent to understand if vH^+-ATPase activity was regulated by $G_{\alpha o}$ in hopes to further resolve the sequence of events occurring within this cascade.

To investigate vH^+-ATPase's influence on the swelling response, isolated synaptic vesicles were administered bafilomycin (a vH^+-ATPase inhibitor) and stimulated to swell via GTP-mastoparan. It was determined that if synaptic vesicle acidification was inhibited, so too was the swelling response (Figure 17 & 22). To further examine the activity of vH^+-ATPases, isolated synaptic vesicles were placed in varying pH environments with bafilomycin and stimulated to swell. When vesicles were in a pH environment that was anything other than neutral pH (pH 7.5), there swelling response was completely inhibited (Figure 17C, D). What was interesting to note was that the swelling response was decreased in the presence of bafilomycin, but not completely abolished (Figure 17A-D, Figure 18). However, bafilomycin did cause a decrease in the rate of swelling response to GTP-mastoparan (Figure 17E). These findings suggested that because the swelling response was not completely inhibited, the vH^+-ATPase is in fact one of the proteins that is activated in the G-protein signaling cascade at the level of the vesicle. Also, because vesicles still swell in response to GTP-mastoparan, even in the presence of bafilomycin, it appears that vH^+-ATPases are located upstream (Figure 20) of aquaporin channels in the signaling cascade and that

www.manaraa.com

proper acidification of secretory vesicles must occur in order for swelling and subsequent expulsion to occur.

As a follow up to these swelling studies, further investigation into all the proteins involved in this vesicular signaling cascade would provide us with a better understanding of the regulatory mechanisms employed during vesicle swelling and expulsion of intravesicular contents. By utilizing a series of inhibitors for the proteins that participate in the swelling response, the sequence of protein channel activation could be elucidated. Additionally, a series of immunoprecipitation experiments could be used to determine which proteins are physically coupled within the vesicle membrane and are most likely activated in succession with one another.

Collectively the present study findings suggest the cell to be even more complex than previously thought. It is clear that there are signaling cascades that occur within organelles of the cell, such as the vesicle. Again, these data reiterate the complexity of the secretory process and how secretion of products from the cell is very tightly regulated. A greater understanding of cell secretion would unfold many mysteries within the cell and provide us with a better understanding of certain disease progression and possible treatment options.

www.manaraa.com

REFERENCES

1. Abu-Hamdah R, Cho WJ, Cho SJ, Jeremic A, Kelly M, Ilie AE, Jena BP. (2004) Regulation of the water channel aquaporin-1: isolation and reconstitution of the regulatory complex. *Cell Biol Int* OU, 7-17.
2. Aguado F, Majo G, Ruiz-Montasell B, LLorens J, Marsal J, Blasi J. (1999) Syntaxin 1A and 1B display distinct distribution patterns in the rat peripheral nervous system. *Neurosc*. 88, 437-446.
3. Bastani B, Purcell H, Hemken P, Trigg D, Gluck S. (1991) Expression and distribution of renal vacuolar proton-translocating adenosine triphosphatase in response to chronic acid and alkali loads in the rat. *J Clin Invest* 88, 126–136.
4. Bastani B, McEnaney S, Yang L, Gluck S. (1994) Adaptation of inner medullary collecting duct vacuolar H-adenosine triphosphatase to chronic acid or alkali loads in the rat. Exp Nephrol 2, 171–175.
5. Baxter JD, Lewicki JA, Gardner DG. (1988) Atrial natriuretic peptide. *Nature Biotechnology* 6, 529-546.
6. Bennett V. (1990). Spectrin-based membrane skeleton: a multipotential adaptor between plasma membrane and cytoplasm. *Physiol Rev 70*, 1029-1065.
7. Bennett K, Calakos N, Scheller RH. (1992) Syntaxin: A synaptic protein implicated in docking of synaptic vesicles at presynaptic active zones. *Science 257*, 255-259.
8. Bradford M. (1976) A rapid and sensitive method for the quantitation of microgram quantities of protein utilizing the principle of protein dye binding. *Anal Biochem* 72, 248–254.
9. Chambrey R, Paillard M, Podevin RA. 1994. Enzymatic and functional evidence

www.manaraa.com

for adaptation of the vacuolar H-ATPase in proximal tubule apical membranes from rats with chronic metabolic acidosis. *J Biol Chem* 269, 3243–3250.

10. Chen Z, Lee JS, Shin L, Cho WJ, Jena BP. (2010) Involvement of β-adrenergic receptor in synaptic vesicle welling and implication in neurotransmitter release. *J Cell Mol Med* Published online.
11. Chernomordik L. (1996) Non-bilayer lipids and biological fusion intermendiates. *Chem Phys Lipids* 81, 203-213.
12. Cho SJ, Abdus Sattar AKM, Jeong EH, Satchi M, Cho JA, Dash S, Mayes MS, Stromer MH, Jena BP. (2002c) Aquaporin 1 regulates GTP-induced rapid gating of water in secretory vesicles. *PNAS* 99, 4720-4724.
13. Cho SJ, Cho J, Jena BP. (2002a) The number of secretory vesicles remains unchanged following exocytosis. *Cell Biol Int* 26, 29-33.
14. Cho SJ, Kelly M, Rognlien KT, Cho JA, Hörber H, Jena BP. (2002d) SNAREs in opposing bilayers interact in a circular array to form conducting pores. *Biophys J* 83, 2522-2527.
15. Cho SJ, Jeftinija K, Glavaski A, Jeftinija S, Jena BP, Anderson LL. (2002e) Structure and dynamics of the fusion pores in live GH-secreting cells revealed using atomic force microscopy. *Endocrinology* 143, 1144–8.
16. Cho SJ, Quinn AS, Stromer MH, Dash S, Cho J, Taatjes DJ, Jena BP. (2002b) Structure and dynamics of the fusion pore in live cells. *Cell Biol Int* 26, 35-42.
17. Cho, SJ, Wakade A, Pappas GD, Jena BP. (2002f). New structure involved in transient membrane fusion and exocytosis. *New York Academy of Science Annals* 971, 254-256.
18. Cho WJ, Jeremic A, Jena BP. (2005a) Size of the supramolecular SNARE

www.manaraa.com

complex: membrane-directed self-assembly. *J Am Chem Soc* 127, 10156-10157.

19. Cho WJ, Jeremic A, Jena BP. (2005b). Direct interaction between SNAP-23 and L-type calcium channel. *J Cellular & Mol Med* 9, 380-386.

20. Cho WJ, Jeremic A, Jin H, Ren G, Jena BP. (2007) Neuronal fusion pore assembly requires membrane cholesterol. *Cell Biol Int* 31, 1301-1308.

21. Cho WJ, Jeremic A, Rognlien KT, Zhvania MG, Lazrishvili I, Tamar B, Jena BP. (2004) Structure, isolation, composition and reconstitution of the neuronal fusion pore. *Cell Biol Int* 28, 699-708.

22. Cho WJ, Ren G, Jena BP. (2008) EM 3D contour maps provide protein assembly at the nanoscale within the neuronal porosome complex. *J Microscopy* 232, 106–111.

23. Collins NC, Thordal-Christensen H, Lipka V, Bau S, Kombrink E, Qui JL, Hücklhoven R, Sten M, Freialdenhoven A, Sommerville SC, Schultze-Lefert P. (2003) SNARE-protein-mediated disease resistance at the plant cell wall. *Nature* 425, 973-977.

24. Cook JD, Cho WJ, Stemmler TL, Jena BP. (2008) Circular Dichroism (CD) spectroscopy of the assembly and disassembly of SNAREs: the proteins involved in membrane fusion in cells. *Chem Phys Lett* 462, 6-9.

25. Faigle W, Colucci-Guyon E, Louvard D, Amigorena S, Galli T. (2000) Vimentin filaments in fibroblasts are a reservoir for SNAP-23, a component of the membrane fusion machinery. *Mol Biol Cell* 11, 3485-3494.

26. Fang X, Gaudette D, Furui T, Mao M, Estrella V, Eder A, Pustilnik T, Sasagawa T, Lapushin R, Yu S, Jaffe RB, Wiener JR, Erickson JR, Mills GB. (2000)

www.manaraa.com

Lysophopholipid growth factors in the initiation, progression, metastases, and management of ovarian cancer. *Annals New York Acad. Sciences* 905, 188-208.

27. Fergestad T, Wu MN, Schulze KL, Lloyd TE, Bellen HJ, Broadie K. (2001) Targeted Mutations in the syntaxin H3 domain specifically disrupt SNARE complex function in synaptic transmission. *J Neurosci* 21, 9142-9150.

28. Füldner H, Stadler H. (1982) 31P-NMR analysis of synaptic vesicles. Status of ATP and internal pH. *Eur J Biochem* 121, 519–524.

29. Goodson HV, Valetti C, Kreis TE. (1997) Motors and membrane traffic. *Curr Opin Cell Biol* 9, 18-28.

30. Gorry PA. (2002). General least-squares smoothing and differentiation by the convolution (Savitzky-Golay) method. *Analytical Chem* 62, 570-573.

31. Han JH, Cao C, Kim SZ, Cho KW, Kim SH. (2003) Decreases in ANP secretion by lysophosphatidylcholine through protein kinase C. *Hypertension* 41, 1380-1385.

32. Hansen NJ, Antonin W, Edwardson JM. (1999) Identification of SNAREs involved in regulated exocytosis in the pancreatic acinar cell. *J Biol Chem* 274, 22871-22876.

33. Hausmann K, Allen RD. (1997) Membranes and microtubules of the excretory apparatus of Paramecium caudatum. *Cytobiologie* 15, 303-320.

34. Hicks B, Parsons S. (1992) Characterization of the P-type and V-type ATPases of cholinergic synaptic vesicles and coupling of nucleotide hydrolysis to acetylcholine transport. *J Neurochem* 58, 1211–1220.

35. Higashijima T, Uzu S, Nakajima T, Ross E. (1988) Mastoparan, a peptide toxin from wasp venom, mimics receptors by activating GTP-binding regulatory

www.manaraa.com

proteins (G proteins). *J Biol Chem* 263, 6491–6494.

36. Jeans AF, Oliver PL, Johnson R, Capogna M, Vikman J, Molnár Z, Babbs A, Partrige CJ, Salehi A, Bengtsson M, Eliasson L, Rorsman P, Davies KE. (2007) A dominant mutation in SNAP25 causes impaired vesicle trafficking, sensorimotor gating, and ataxia in the blind-drunk mouse. *PNAS* 104, 2431-2436.

37. Jena BP. (2004) Discovery of the porosome: revealing the molecular mechanism of secretion and membrane fusion in cells. *J Cellular & Mol Med* 8, 1-21.

38. Jena BP. (2007) Secretion machinery at the cell plasma membrane. *Current Opinion Struc Biol* 17, 437-443.

39. Jena BP. (2009) Porosome: the secretory portal in cells. *Biochemistry* 49, 4009-4018.

40. Jena BP. (2011) Porosome: the universal secretory portal in cells. *Biomed Rev* 21, 1-15.

41. Jena BP, Cho SJ, Jeremic A, Stromer MH, Abu-Hamdah R. (2003) Structure and composition of the fusion pore. *Biophys J* 84, 1-7.

42. Jena BP, Schneider SW, Geibel JP, Webster P, Oberleithner H, Sritharan KC. (1997) Gi regulation of secretory vesicle swelling examined by atomic force microscopy. *Proc Natl Acad Sci USA* 94, 13317–13322.

43. Jeremic A, Kelly M, Cho J, Cho SJ, Stromer MH, Jena BP. (2003) Reconstituted fusion pore. *Biophys J* 85, 2035-2043.

44. Jeremic A, Cho WJ, Jena BP. (2004) Membrane fusion: what may transpire at the atomic level. *J Biol Phys Chem* 4, 139-142.

45. Jeremic A, Cho WJ, Jena BP. (2005) Involvement of water channels in synaptic

www.manaraa.com

vesicle swelling. *Exp Biol Med* 230, 674-680.

46. Jeremic A, Quinn AS, Cho WJ, Taatjes, Jena BP. (2006) Energy-dependent disassembly of self-assembled SNARE complex: observation at nanometer resolution using atomic force microscopy. *J Am Chem Soc* 128, 26-27.

47. Joiner KA, Ross DS. (2002) Secretory traffic in the eukaryotic parasite *Toxoplasma gondii*: less is more. *J Cell Biol* 157, 557-563.

48. Jougasaki M, Kugiyama K, Saito Y, Nakao K, Imura H, Yasue H. (1992) Suppression of endothelin-1 secretion by lysophosphatidylcholine in oxidized low density lipoprotein in cultured vascular endothelial cells. *Circ Res* 71, 614-619.

49. Kelly ML, Cho WJ, Jeremic A, Abu-Hamdah R, Jena BP. (2004) Vesicle swelling regulates expulsion during secretion. *Cell Biol Int* 28, 709-716.

50. Konrad R, Young R, Record R, Smith R, Butkerait P, Manning D, Jarett L, Wolf B. (1995) The heterotrimeric G-protein Gi is localized to the insulin secretory granules of beta-cells and is involved in insulin exocytosis. *J Biol Chem* 270, 12869–12876.

51. Kubori T, Matsushima Y, Nakamura D, Uralil J, Lara-Tejero M, Sukhan A, Galán JE, Aizawa SI. (1998) Supramolecular structure of the Salmonella typhimurium type III protein secretion system. *Science* 280, 602-605.

52. Lang T, Bruns D, Wenzel D, Riedel D, Holroyd P, Thiele L, Jahn R. (2001) SNAREs are concentrated in cholesterol-dependent clusters that define docking and fusion sites for exocytosis. *EMBO J* 20, 2202-2213.

53. Lee JS, Cho WJ, Jeftinija K, Jeftinija S, Jena BP. (2009) Porosome in astrocytes. *J Cell Mol Med* 13, 365-372.

54. Littleton JT, Bernard RJO, Titus SA, Slind J, Chapman ER, Ganetzky B. (2001)

www.manaraa.com

SNARE-complex disassembly by NSF follows synaptic-vesicle fusion. *Pro Natl Acad Sci* 98, 12233-11238.

55. Malhotra V, Orci L, Glick BK, Block MR, Rothman JE. (1988) Role of an N-ethylmaleimide-sensitive transport component in promoting fusion of transport vesicles with cisternae of the Golgi stack. *Cell 54*,221-227.

56. McIntosh TJ, Simon SA. (2006) Roles of bilayer material properties in function and distribution of membrane proteins. *Annu Rev Biophys Biomol Struct* 35,177-198.

57. McMahon HT, Gallop JL. (2005) Membrane curvature and mechanisms of dynamic cell membrane remodeling. *Nature* 438, 590-596.

58. Michaelson D, Angel I. (1980) Determination of pH in cholinergic synaptic vesicles: its effect on storage and release of acetylcholine. *Life Sci* 27, 39–44.

59. Mima J, Wickner W. (2009) Complex lipid requirements for SNARE- and SNARE chaperone-dependent membrane fusion. *J Biol Chem* 284, 27114-27122.

60. Mirnics K, Middleton FA, Marquez A, Lewis DA, Levitt P. (2000) Molecular characterization of schizophrenia viewed by microarray analysis of gene expression in the prefrontal cortex. *Neuron* 28, 53-67.

61. Mitter D, Reisinger C, Hinz B, Hollmann S, Yelamanchili SV, Treiber-Held S, Ohm TG, Herrmann A, Ahnert-Hilger G. (2003) The synaptophysin/synaptobrevin interaction critically depends on the cholesterol content. *J Neurochem* 84, 35-52.

62. Morel N, Dunant Y, Israël M. (2001) Neurotransmitter release through the V0 sector of V-ATPase. *J. Neurochem* 79, 485-488.

www.manaraa.com

63. Nakano M, Nogami S, Sato S, Terano A, Shirataki H. (2001) Interaction of syntaxin with α-fodrin, a major component of the submembranous cytoskeleton. *Biochem Biophys Res Commun* 288, 468-475.

64. Nomura DK, Long JZ, Niessen S, Hoover HS, Ng S-W, Cravatt BF. (2010) Monoacylglycerol lipase regulates a fatty acid network that promotes cancer pathogenesis. *Cell 140*, 49-61.

65. Ohyama A, Komiya Y, Igarashi M. (2001) Globular tail of myosin-V is bound to vamp/synaptobrevin. *Biochem Biophys Res Commun* 280, 988-991.

66. Oyler GA, Higgins GA, Hart RA, Battenbarg M, Bloom FE, Wilson MC. (1989) The identification of a novel synaptosomal associated protein, SNAP-25, differentially expressed by neuronal subpopulations. *J Cell Biol 109*, 3039-3052.

67. Paumet F, Wesolowski J, Garcia-Diaz A, Delevoye C, Aulner N, Shuman HA, Subtil A, Rothman JE. (2009) Intracellular bacteria encode inhibitory SNARE-like proteins. Published Online (www.plosone.org).

68. Peng XR, Yao X, Chow DC, Forte JG, Bennette MK. (1997) Association of syntaxin 3 and vesicle-associated membrane protein (VAMP) with H+/K+-ATPase-containing tubulovesicles in gastric parietal cells. *Mol Biol Cell* 8, 399-407.

69. Peters C, Bayer M, Bühler S, Andersen J, Mann M, Mayer A. (2001) Trans-complex formation by proteolipid channels in the terminal phase of membrane fusion. *Nature* 409, 581–588.

70. Provencher SW, Glockner J. (1981) Estimation of globular protein secondary structure from circular dichroism. *Biochem* 20, 33-37.

71. Ravichandran V, Chawla A, Roche PA. (1996) Identification of a novel syntaxin

www.manaraa.com

and synaptobrevin/VAMP-binding protein, SNAP-23, expressed in non-neuronal tissues. *J Biol Chem* 271, 13300-13303.

72. Sabatinin BL, Regehr WG. (1996) Timing of neurotransmission at fast synapse in the mammalian brain. *Nature* 384, 170-172.

73. Santos T, Souza D, Tasca C. (2005) GTP uptake into rat synaptic vesicles. *Brain Res* 1070, 71–76.

74. Schneider SW, Sritharan KC, Geibel JP, Oberleithner H, Jena BP. (1997) Surface dynamics in living acinar cells imaged by atomic force microscopy: identification of plasma membrane structures involved in exocytosis. *Proc Natl Acad Sci USA* 85, 4538-4542.

75. Shin L, Basi N, Jeremic A, Lee JS, Cho WJ, Chen ZH, Abu-Hamdah R, Oupicky D, Jena BP. (2010) Involvement of vH+-ATPase in synaptic vesicle swelling. *J Neurosci Res* 88, 95-101.

76. Siksou L, Rostaing P, Lechaire JP, Boudier T, Ohtsuka T, Fejtova A, Kao HT, Greengard P, Gundelfinger ED, Triller A, Marty S. (2007) Three-dimensional architecture of presynaptic terminal cytomatrix. *J Neurosci* 27, 6868–6877.

77. Sprecher E, Ishida-Yamamoto A, Mizrah-Koren M, Rapaport D, Goldsher D, Indleman M, Topaz O, Chefetz I, Keren H, O'Brien TJ, Bercovich D, Shaley S, Geiger D, Bergman R, Horowitz M, Mandel H. (2005) A mutation in SNAP29, coding for a SNARE protein involved in tracellular trafficking, causes a novel neurocutaneous syndrome characterized by cerebral dysgenesis, neuropathy, ichthyosis, and palmoplantar keratoderma. *Am J Hum Genet* 77, 242-251.

78. Spector AA, Yorek MA. (1985) Membrane lipid composition and cellular function. *J Lipid Res* 26, 1015-1035.

www.manaraa.com

79. Stadler H, Tsukita S. (1984) Synaptic vesicles contain an ATP-dependent proton pump and show ‘‘knob-like’’ protrusions on their surface. *EMBO J* 3, 3333–3337.

80. Sutphen R, Xu Y, Wilbanks GD, Fiorica J, Grendys Jr EC, LaPolla JP, Arango H, Hoffman MS, Martino M, Wakeley K, Griffin D, Blanco RW, Cantor AB, Xiao Y, Krischer JP. (2004) Lysophospholipids are potential biomarkers of ovarian cancer. *Cancer Epidemiol Biomarkers Prev* 13, 1185-1191.

81. Sutton RB, Fasshauer D, Jahn R, Brunger AT. (1998) Crystal structure of a SNARE complex involved in synaptic exocytosis at 2.4Å resolution. *Nature* 395, 347-353.

82. Trimble WS, Cowam DM, Scheller RH. (1988) VAMP-1: A synaptic vesicle-associated integral membrane protein. *Proc Natl Acad Sci USA 85*, 4538-4542.

83. Trikha S, Lee EC, Jeremic AM (2010) Cell Secretion: Current Structural and Biochemical Insights. *The Scientific World J* 10, 2054-2069.

84. Vitale N, Mukai H, Rouot B, Thierse´ D, Aunis D, Bader M-F. (1993) Exocytosis in chromaffin cells. Possible involvement of the heterotrimeric GTP-binding protein G(o). *J Biol Chem* 268, 14715–14723.

85. Wang W, Yang L, Huang HW. (2007) Evidence of cholesterol accumulated in high curvature regions: implication to the curvature elastic energy for lipid mixtures. *Biophys J* 92, 2819-2830.

86. Weber T, Zemelman BV, McNew JA, Westermann B, Gmachi M, Parlati F, Söllner TH, Rothman JE. (1998) SNAREpins: minimal machinery for membrane fusion. *Cell* 92,759 –772.

87. Weingarten R, Ransnas L, Mueller H, Sklar L, Bokoch G. (1990) Mastoparan interacts with the carboxyl terminus of the alpha subunit of Gi. *J Biol Chem* 265,

www.manaraa.com

11044–11049.

88. White JG. (1999) Platelet secretory process. *Blood* 93, 2422-2425.

89. White JG, Clawson CC. (1980) The surface-connected canalicular system of blood platelets –a fenestrated membrane system. *Am J Pathol* 101, 353-359.

90. Yasui M, Hazama A, Kwon TH, Nielsen S, Guggino W B, Agre P. (1999) Rapid gating and anion permeability of an intracellular aquaporin. *Nature (London)* 402, 184–187.

91. Zamir O, Charlton MP. (2006) Cholesterol and synaptic transmitter release at crayfish neuromuscular junctions. *J Physiol* 571, 83-99.

92. Zimmerberg J, Chernomordik LV. (2005) Synaptic membranes bend to the will of a neurotoxin. *Science* 310, 1626-1627.

www.manaraa.com

ABSTRACT

MOLECULAR MECHANISMS OF SNARE ASSEMBLY AND EXPULSION OF INTRAVESICULAR CONTENTS IN CELL SECRETION

by

LEAH J SHIN-ZHANG

August 2011

Advisor: Dr. Bhanu Jena

Major: Physiology

Degree: Doctor of Philosophy

For nearly half a century, it was believed that during cell secretion, membrane-bound secretory vesicles completely merge at the cell plasma membrane resulting in the diffusion of intra-vesicular contents to the cell exterior and the compensatory retrieval of the excess membrane by endocytosis. This explanation made no sense or logic, since following cell secretion partially empty vesicles accumulate as demonstrated in electron micrographs. Furthermore, with the 'all or none' mechanism of cell secretion by complete merger of secretory vesicle membrane at the cell plasma membrane, the cell is left with little regulation and control of the amount of content release. Moreover, it makes no sense for mammalian cells to possess an 'all or none' mechanism of cell secretion, when even single-cell organisms have developed specialized and sophisticated secretory machinery, such as the secretion apparatus of Toxoplasma gondii, the contractile vacuoles in paramecium, or the various types of secretory structures in bacteria. This conundrum in the molecular mechanism of cell secretion was finally resolved in 1997 following discovery of the 'Porosome', the universal secretory machinery in cells. Porosomes are supramolecular lipoprotein structures at

www.manaraa.com

the cell plasma membrane, where membrane-bound secretory vesicles transiently dock and fuse to release inravesicular contents to the outside during cell secretion. In the past decade, the composition of the porosome, its structure and dynamics at nanometer resolution and in real time, and its functional reconstitution into artificial lipid membrane, have been elucidated. Three soluble *N*-ethylmaleimide-sensitive factor (NSF)-attachment protein receptors called SNAREs, have been implicated in membrane fusion in cells. For example in neurons, target membrane proteins SNAP-25 and syntaxin (t-SNARE) present at the porosome base, and a synaptic vesicle-associated membrane protein (v-SNARE), are part of the conserved protein complex involved in fusion of synaptic vesicle membrane at the porosome. Studies demonstrate that t-SNAREs and v-SNAREs, when present in opposing lipid membrane, interact in a circular array, and in the presence of calcium, form conducting channels. The interaction of t-SNARE and v-SNARE proteins to form conducting channels is strictly dependent on the presence of these proteins in opposing membrane. Following stimulation of cell secretion, it has been demonstrated that secretory vesicles swell via rapid transport of water and ions, and the intravesicular pressure thus created enables the expulsion of vesicular contents from the cell via the SNARE channel and the porosome. The focus of the present study was to understand at the molecular level, membrane-associated t-/v-SNARE assembly and secretory vesicle swelling involved in cell secretion. Using t- and v-SNARE reconstituted proteoliposomes, and isolated secretory vesicles, the present study was conducted employing various biochemical and biophysical approaches. The results from this work were published in seven research papers, and provide a molecular understanding of both t-/v-SNARE assembly and secretory vesicle swelling during cell secretion.

www.manaraa.com

AUTOBIOGRAPHICAL STATEMENT

LEAH J SHIN-ZHANG

Education:

Undergraduate: The University of Michigan
Ann Arbor, Michigan
Major: Psychology – Bachelor of Science 2005

Graduate: Wayne State University
Detroit, Michigan
Major: Physiology – Ph.D. (pending)

Selected Publications:

1. Cho WJ, **Shin L**, Ren G, Jena BP. Structure of membrane-associated neuronal SNARE complex: implication in neurotransmitter release. *J Cell Mol Med*. 2009 Oct;13(10):4161-5. Epub 2009 Sep 8.

2. **Shin L**, Basi N, Jeremic A, Lee JS, Cho WJ, Chen Z, Abu-Hamdah R, Oupicky D, Jena BP. Involvement of vH(+)-ATPase in synaptic vesicle swelling. *J Neurosci Res*. 2010 Jan;88(1):95-101.

3. **Shin L**, Cho WJ, Cook JD, Stemmler TL, Jena BP. Membrane lipids influence protein complex assembly-disassembly. *J Am Chem Soc*. 2010 Apr 28;132(16):5596-7.

4. Lee JS, Cho WJ, **Shin L**, Jena BP. Involvement of cholesterol in synaptic vesicle swelling. *Exp Biol Med* (Maywood). 2010 Apr;235(4):470-7.

5. Cho WJ, Lee JS, Zhang L, Ren G, **Shin L**, Manke CW, Potoff J, Kotaria N, Zhvania MG, Jena BP. Membrane-directed molecular assembly of the neuronal SNARE complex. *J Cell Mol Med*. 2011 Jan;15(1):31-7. doi: 10.1111/j.1582-4934.2010.01152.x.

6. Chen ZH, Lee JS, **Shin L**, Cho WJ, Jena BP. Involvement of β-adrenergic receptor in synaptic vesicle swelling and implication in neurotransmitter release. *J Cell Mol Med*. 2011 Mar;15(3):572-6. doi: 10.1111/j.1582-4934.2010.01026.x.

www.manaraa.com